



Contents lists available at ScienceDirect

Quaternary International

journal homepage: www.elsevier.com/locate/quaint

ESR dating of Middle Pleistocene archaeo-paleontological sites from the Manzanares and Jarama river valleys (Madrid basin, Spain)

Davinia Moreno ^{a,*}, Mathieu Duval ^b, Susana Rubio-Jara ^c, Joaquín Panera ^a, Jean Jacques Bahain ^d, Qingfeng Shao ^e, Alfredo Pérez-González ^a, Christophe Falguères ^d

^a Centro Nacional de Investigación sobre la Evolución Humana (CENIEH), Paseo Sierra de Atapuerca, 3, 09002, Burgos, Spain

^b Australian Research Centre of Human Evolution (ARCHE), Environmental Futures Research Institute (EFRI), Griffith University, 170 Kessels Road, Nathan, QLD 4111, Australia

^c Instituto de Evolución en África (IDEA), Museo de San Isidro, Plaza de San Andrés, 2, Madrid, Spain

^d Département de Préhistoire, Muséum National d'Histoire Naturelle, UMR 7194, 1, Rue René Panhard, 75013, Paris, France

^e College of Geographical Science, Nanjing Normal University, Nanjing, 210023, China

ARTICLE INFO

Article history:

Received 26 April 2017

Received in revised form

21 August 2017

Accepted 8 September 2017

Available online xxx

Keywords:

Electron Spin Resonance (ESR) dating

Quartz

Ungulate teeth

Fluvial deposits

Manzanares and Jarama valley

Middle Pleistocene

ABSTRACT

In this work, three important Pleistocene sites of the Madrid basin located close to the junction of the Manzanares (PRERESA site) and the Jarama (Valdocarros site and Maresa quarry) rivers have been studied in order to improve the existing chronological framework of the basin and to clarify the geological evolution of these fluvial systems and their relationship with human occupations. To do so, Electron Spin Resonance (ESR) dating was applied to four fossil teeth and nine optically bleached quartz grain samples. Most of the obtained dates are consistent with the existing preliminary age estimates by biostratigraphy, luminescence (OSL and TL) or Amino Acid Racemization (AAR) dating. This ESR dating study suggests an age of Late Middle Pleistocene (early MIS6) for PRERESA site. At the Jarama valley (Valdocarros site and Maresa quarry), the Arganda I unit could be correlated to the MIS 9 and MIS10, the Arganda II unit seems to belong to MIS8 and MIS7 and the Arganda III to the MIS6.

© 2017 Elsevier Ltd and INQUA. All rights reserved.

1. Introduction

Since the first discovery in 1862 of lithic industry in association with elephant bones at Cerro de San Isidro (Prado, 1864), dozens of archaeo-paleontological sites have been discovered along the Manzanares and Jarama rivers (Panera and Rubio-Jara, 2002) in the central sector of the Madrid Neogene Basin (Fig. 1a). This high density of preserved sites seems to be related with a synsedimentary subsidence process due to the karstic dissolution of the gypsum in the substratum which favored the accumulation of fluvial sediments and a good conservation of both fauna remains and lithic industry (Pérez-González, 1971, 1980; Rubio-Jara et al., 2002). Establishing a chronological framework for this region is crucial to understand the Quaternary evolution of these fluvial systems as well as to comprehend the rich archaeo-paleontological record located in their fluvial terraces. For a long time, the

chronological data have been derived from micro- and macro-mammals assemblages (Sesé and Soto, 2000; Sesé et al., 2011a, 2011b) and stone tools technology (Santonja et al., 1980), but the available data base on numerical ages for the central sector of the Madrid basin has significantly increased during the last years. A good compilation of all the available published numerical age-data on the fluvial sequences in the Madrid Basin can be found in Silva et al. (2016) and in Rubio-Jara et al. (2016). Hence, the present-day chronostratigraphic framework of this region for terraces down to +40 m above the present channel is based on amino acid racemization (AAR) (Panera et al., 2011), luminescence (TL and OSL) (Pérez-González et al., 2008) paleomagnetism (Pérez-González et al., 2013) and radiocarbon dating (Wolf et al., 2013).

In order to improve and refine the existing chronostratigraphic framework, the Electron Spin Resonance (ESR) dating has been applied to four fossil teeth and nine optically bleached quartz grains samples coming from two archaeological sites and a sand/gravel quarry located within fluvial deposits from the Manzanares and Jarama river terrace systems (Madrid Basin).

* Corresponding author.

E-mail address: davinia.moreno@cenieh.es (D. Moreno).

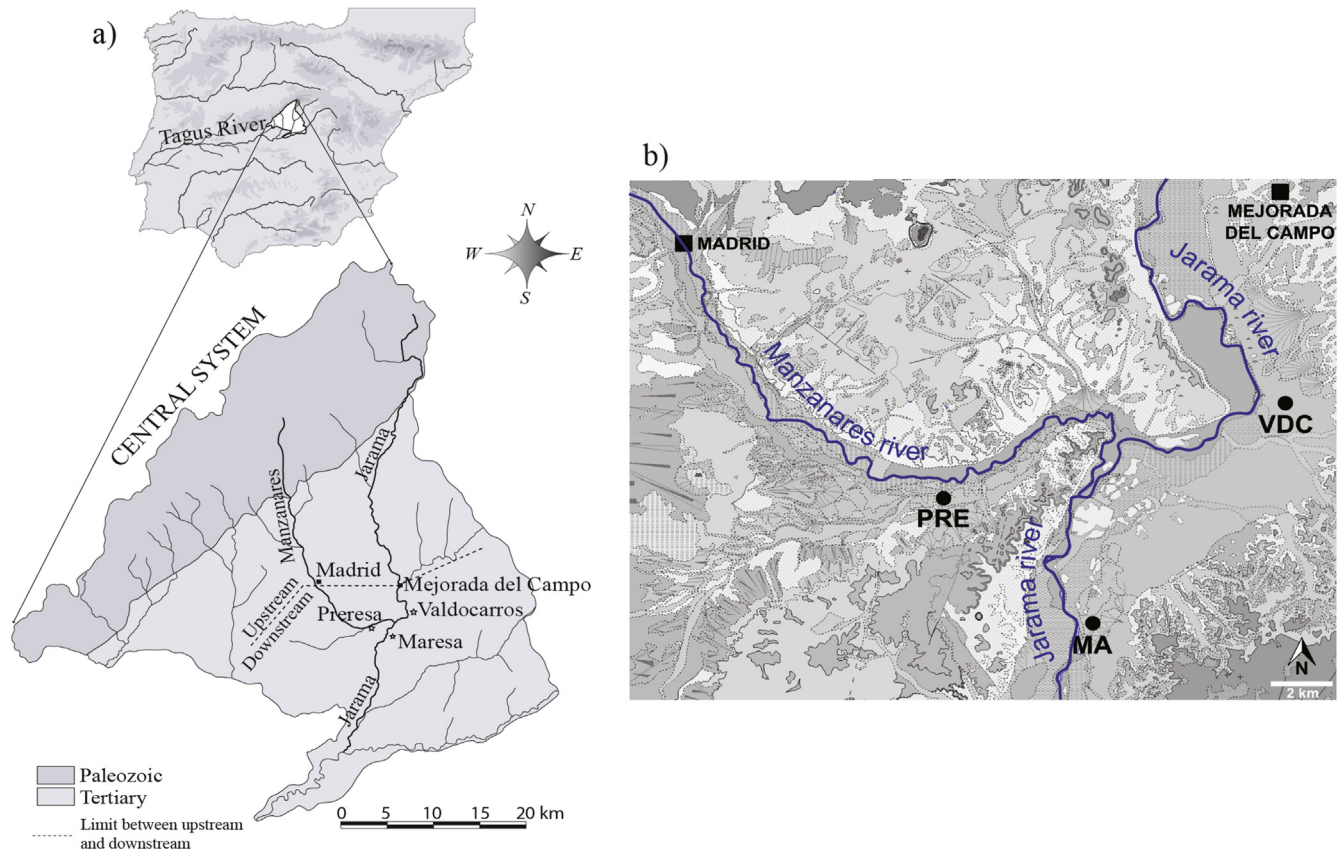


Fig. 1. a) General scheme of the Madrid Basin and its hydrographical network. b) Location of the three studied archaeological sites: Preresa (PRE) in the Manzanares valley; Valdocarros (VDC) and Maresa (MA) in the Jarama valley located upstream and downstream of the confluence with the Manzanares river, respectively. This map has been obtained from <http://igme.maps.arcgis.com/> where the legend and the complete map of the region can be consulted.

2. The Madrid Basin

The Madrid Basin is an intracratonic and triangular basin bounded on its three sides by Tertiary mountain ranges: the Spanish Central system in the north, the Toledo Mountains in the south and the Iberian range in the east (Fig. 1a) (De Vicente et al., 1996). This basin is over 20,000 km² and was filled by Tertiary sediments between 2000 and 3500 m thick. Due to its strategic location between three mountain ranges which have a different structures and Tertiary geological evolutions, the Madrid Basin shows a complex deformational history as a result of differential compressive strains from the North and South during Alpine movements. Concurrently with this complicated tectonic activity and following the main fault lineages, an important hydrographic network was developed in this area (Silva et al., 1988; Giner et al., 1996) corresponding with the upstream part of the Tagus drainage basin which is composed of several water bodies. The materials that infilled the basin are mainly represented by conglomerates with limestone and quartzite boulders, sandstones, clays marls, limestones and gypsums (De Vicente and Muñoz-Martín, 2013).

Two of the most important water bodies in the Madrid Basin are the Jarama and Manzanares rivers. Their alluvial terraces systems show a high number of terraces and are rich in palaeontological and archaeological sites. The Quaternary evolution of the Jarama and Manzanares fluvial systems has been controlled by synsedimentary subsidence due to the karstification of the evaporitic bedrock. This phenomenon is a well-known process in the large tertiary continental basins in Spain (Benito et al., 2000). It produces anomalous

morphostratigraphical features because alluvial systems counter-balance subsidence by aggradation to maintain a dynamic equilibrium profile of the alluvial surface. The replication of the synsedimentary subsidence through a particular area results in significant thickening of fluvial deposits and superposition of the deposits correlative to different terrace levels (Pérez-González, 1971).

2.1. Manzanares river valley

The Manzanares River has its source in the Guadarrama mountain range and flows in the Jarama River 92 km later. Upstream from the city of Madrid the river follows an N-S direction until the confluence with the Butarque stream where the valley progressively turns into an NW-SE arched direction until joining the Jarama River (Fig. 1b). The upstream reach of the valley exhibits thirteen levels of stepped alluvial terraces (T1-T13) with a maximum relative height of +95 m and a minimum relative height of +4–5 m above the present thalweg (Pérez-González, 1994) (Table 1). These alluvial deposits are 3–4 m thick and consist of sands and gravels overlain by floodplain fine-grained deposits with well-developed soils (Goy et al., 1989). The lower reach of the valley is carved in evaporitic bedrock and is affected by synsedimentary subsidence which normally displays thickened fluvial sequences and creates a system of overlapped (complex) terraces. The so-called *Complex Terrace of Butarque* (hereafter CTB) by Goy et al. (1989), also called *Complex Terrace of Manzanares* (TCMZ) (Silva, 2003), is the most extensive terrace level developed in the lower reach of the valley and it could be composed of at least two terraces,

namely T9 (+18–20 m) and T8 (+25–30 m) (Pérez-González and Uribealra, 2002). Since the mid-20th, many palaeontological and/or archaeological sites have been identified and excavated within the deposits associated to the CTB terrace (Panera and Rubio-Jara, 2002), which is contrasting with fluvial terraces located higher than +40 m above the present thalweg where bone remains and lithic artefacts are mostly absent (Rubio-Jara et al., 2016).

The chronology of the terrace sequence at the Manzanares river valley has been traditionally derived from regional relative height correlations, bio- and archaeo-stratigraphy (Table 1). In this way, the fluvial levels between T12 and T9 (+8 m and +20 m) have been tentatively ascribed to the Upper Pleistocene, while terraces between T9 and T4 (+20 m and +60 m) to the Middle Pleistocene and those higher than +60 m (T4–T1) to the Lower Pleistocene (Pérez-González and Uribealra, 2002; Rubio-Jara et al., 2016). The CTB has traditionally been ascribed to the Middle Pleistocene, which is corroborated by the abundant remains of large mammals such as *Elephas* (*Palaeoloxodon*) *antiquus*, *Dicerorhinus hemitoechus*, *Bos primigenius*, *Equus caballus*, *Cervus elaphus* (Sesé and Soto, 2000) and the Acheulean industry found at the bottom of the terrace (Rubio-Jara et al., 2016). However, the available numerical dates, taken from different sites spread along the CTB, indicate that the T9 (+18–20 m) level may include the Middle-Late Pleistocene boundary (Pérez-González et al., 2008; Silva et al., 2008, 2012; Domínguez-Alonso et al., 2009; Laplana et al., 2015). In the Arriaga sand quarry, also located within the CTB, two thermoluminescence (TL) dates provided minimum ages of 133 ka and 134 ka (Silva et al., 2011, 2012) and may position the lower outcrop of the CTB within the final part of the Middle Pleistocene (Sesé and López-Martínez, 2013). At EDAR Culebro 1 site, an OSL date of 121 ± 7 ka and two AAR dates on an *Equus* sp. molar (133 ± 28 and 105 ± 10 ka) have been obtained (Manzano et al., 2010). At Los Estragales site, the lower alluvial sequence has provided one Optically Stimulated Luminescence (OSL: $107 \pm 39/-22$ ka) and one Thermoluminescence (TL: 122 ± 11 ka) ages for the bottom of the CTB. Another OSL date for the top of the sequence, 91 ± 9 ka (Pérez-González et al., 2008) was calculated. The site of PRERESA has been dated to 84 ± 5.6 ka by OSL on feldspar grains (Yravedra et al., 2012; Panera et al., 2014). The T10 (+12–15 m) level has also provided two TL ages: 40 ± 3 ka (Pérez-González et al., 2008) and 40 ± 5 ka at the E.T.B site (Domínguez-Alonso et al., 2009).

2.2. Jarama river valley

The Jarama River has its source in the Sierra de Guadarrama and after 150 km crossing the Madrid Basin southwards, flows into the Tagus River. This is an asymmetric valley which exhibits gypsum cliffs along the right bank and a sequence of alluvial terraces on the left bank. Downstream of Mejorada del Campo and upstream of Arganda del Rey, a sequence of fifteen stepped alluvial terraces (T1–T15) with a maximum of +140–145 m and a minimum of +4–5 m relative height (Pérez-González, 1994) above the present thalweg (Table 1). In this area, only the alluvial terraces higher than +40 m are stepped. The lower terraces are affected by syndimentary subsidence processes resulting to the *Complex Terrace of Arganda* (hereafter CTA). The CTA is composed of four alluvial sequences called Arganda I, II, III and IV (from the bottom to the top) that can reach up to 40–50 m in thickness (Pérez-González, 1971, 1980; 1994) (Fig. 2). Arganda I (T12: +30–32 m) is characterized by a succession of sandy levels locally cut by thin gravel beds and all overlain by floodplain silt-clay deposits while Arganda II (T13: +23–24 m) is composed by a series of gravel bars. Arganda III (T14: +18–20 m) is a new alluvial terrace, enclosed ~5 m in Arganda II and composed of gravel bars cemented by calcium

carbonate. Arganda IV is constituted by slope deposits coming from the nearby Miocene and Quaternary reliefs (Pérez-González, 1980). On the CTA deposits, numerous palaeontological and archaeological sites have been discovered such as Áridos 1 and 2, HAT, Valdocarros and Maresa (Santonja et al., 1980; Panera et al., 2005; Panera, 2009; Rubio-Jara et al., 2016).

The chronology of the terrace sequence at the Jarama river valley has been established on the combination of regional relative height correlations, biostratigraphy, numerical dating and palaeomagnetism (Table 1). The CTA numerical time frame has been established by a combination of biostratigraphy (López-Martínez, 1980; Sesé et al., 2011a,b) with amino-acid racemization (AAR) dating (Panera et al., 2011). In Arganda I and Arganda II, the micromammals associations from Áridos 1 and Valdocarros, respectively, suggest a late Middle Pleistocene age for these deposits. The AAR results indicate that the Arganda I unit (332 ± 38 and 379 ± 45 ka at Maresa site) spans the last part of MIS 11 or early MIS 9, which is coherent with the micromammals association. The Arganda II unit at Valdocarros site yielded three ages. Two of them (254 ± 47 and 262 ± 07 ka) are internally consistent and in agreement with the biostratigraphy and may correspond with an interstadial within the cold stage MIS 8 or the MIS 8/7 transition (Blain et al., 2012). The third date (174 ± 20 ka) is however, significantly younger and does not overlap with the other two (Panera et al., 2011). Because of the hardening of sediments in Arganda III unit no micromammal remains have been found and no numerical dates have been obtained. In Arganda IV several numerical ages obtained by TL ($112 \pm 36/-22$ ka and $85 \pm 18-13$ ka at Torreblanca; $74 \pm 16-12$ ka at HAT) and OSL (80 ± 7 ka at Valdocarros and 74 ± 5 ka at Maresa) suggest an Upper Pleistocene age for this unit, which may correlate with MIS 5 (Panera et al., 2011). The Brunhes-Matuyama boundary (0.780 Ma) has been recorded between the terrace T8 (+60–65 m; *reverse polarity*) and the T9 (+55–60 m; *normal polarity*) (Pérez-González et al., 2013). This is consistent with the results obtained on Arlanzón river valley (Duero basin) which show an Electron Spin Resonance (ESR) date of at least 780 ka and *reverse polarity* for T4 (+60–67 m) and an ESR age of 670 ka and *normal polarity* for T5 (+50–54 m) (Benito-Calvo et al., 2008; Moreno et al., 2012).

3. The archaeological sites studied

The sites studied in this paper are PRERESA in the Manzanares valley and Valdocarros and Maresa in the Jarama valley located upstream and downstream of the confluence with the Manzanares River, respectively (Fig. 1b).

3.1. PRERESA (PRE) site

The PRERESA site was discovered in 2003, 5.5 m below the top of the CTB, thanks to archaeological surveys (Panera et al., 2009). The stratigraphy of the site includes, from the bottom to the top, sandy bars and channel fills floodplain sediments followed by sandy bars with gravels showing crossed-stratigraphy topped by a sequence of clays and muds (Fig. 3I). An area of 255 m² was excavated in a 30 cm-thick greenish clayey facies. 754 lithic pieces were recorded, all made of flint apart from six pieces of quartz. The lack of macro-tools and the low occurrence of retouched tools are remarkable. Among these, the most common are retouched flakes, denticulates and compound tools. A scraper and a burin were also recorded. The presence of knapping remains demonstrates that these flakes were shaped *in situ* (Rubio-Jara, 2011). Lithic remains are associated with an important association of macromammals such as *Haploidoceros mediterraneus*, *Vulpes vulpes*, *Lynx pardinus*, *Meles meles*, *Canis lupus*, *Proboscidea indet.*, *Equus* sp., *Cervus elaphus*, *Dama* sp., *Capreolus*

Table 1

Terrace sequences of the Manzanares and Jarama valleys displaying the maximum number of terrace levels recorded in the work area with indication of the relative height in m, above the present thalweg (FP: floodplain) (Pérez-González, 1994; Rubio-Jara et al., 2016) along with palaeomagnetic, paleontological data and numerical ages: TL (Thermoluminescence), OSL (Optically Stimulated Luminescence) and AAR (Amino Acid Racemisation) (Pérez-González et al., 2008; Domínguez-Alonso et al., 2009; Manzano et al., 2010; Panera et al., 2011, 2014; Silva et al., 2012; Yravedra et al., 2012).

		Manzanares valley							Jarama valley				Techno- Complex				
		Terraces (m)		Numerical ages (ka)					Terraces (m)		Numerical ages (ka)				Magnetostratigraphy		
				Arriaga	Edar Culebro	Estragales	E.T.B.	PRERESA			Valdocarros	Maresa					
				TL	TL	AAR	OSL/TL	TL			OSL	AAR				AAR	
Holocene		FP	+1-1,5														
Pleistocene	Upper Pleistocene	T13	+4-5							T15	+4-5						
		T12	+8														
		T11	+10														
		T10	+12-15														
	Middle Pleistocene	T9	+18-20	>133	121 ± 7	105 ± 10	122 ± 11		84 ± 5.6	T14	+18-20			Middle Paleolithic Acheulean			
			≈ CTB	134 ± 50		133 ± 28	107 + 39/-22	91 ± 9			≈ Arganda III CTA						
		Middle Pleistocene	T8	+25-30						T13	+23-24	254 ± 47			Acheulean		
				≈ CTB?							≈ Arganda II CTA	262 ± 07					
												174 ± 20					
	Lower Pleistocene	T7	+35-40							T12	+30-32		332 ± 38				
										≈ Arganda I CTA		379 ± 45					
									T11	+40-41							
		T6	+44-46							T10	+52-53				Acheulean?		
		T5	+52-54							T9	+55-60						
		Lower Pleistocene	T4	+60							T8	+60-65					
			T3	+68-72							T7	+74					
T2			+80-85							T6	+84-86						
T1			+95							T5	+92						
										T4	+100-104						
								T3	+110-114								
								T2	+125-130								
								T1	+140-145								

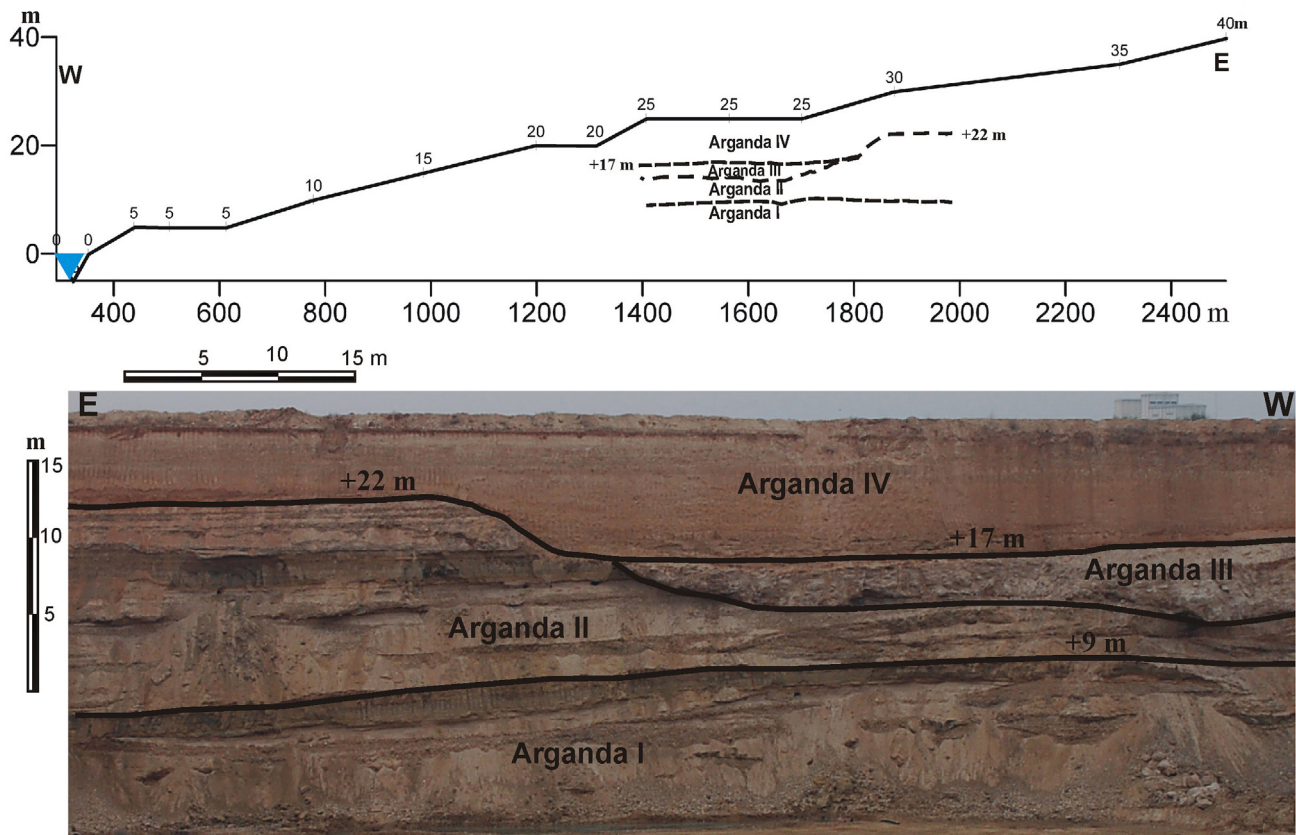


Fig. 2. Jarama river valley cross-section and TCA section at Valdocarros site where the four Arganda units (I, II, III and IV) can be observed. (Modified from Panera et al., 2011).

capreolus and *Bos primigenius* (Panera et al., 2014) in addition to micromammal and herpetofauna remains. The small-mammal assemblage mainly includes Erinaceomorpha: *Erinaceus europaeus*; Soricomorpha: *Crocidura russula*; Chiroptera: *Rhinolophus ferrumequinum*; Rodentia: *Eliomys quercinus*, *Apodemus* sp., *Cricetulus* (*Allocricetus*) *bursae*, *Arvicola* aff. *sapidus*, *Microtus cabreræ*, *Microtus duodecimcostatus*; Lagomorpha: *Oryctolagus cuniculus* (Sesé et al., 2011a). The herpetological assemblage consists of *Pelobates cultripedes*, *Pelodytes*, sp., *Bufo bufo*, *Bufo calamita*, *Hyla* sp., *Pelophylax perezi*, *Natri maura*, *Vipera tatastei* (Blain et al., 2013). According to the presence of *Microtus cabreræ* and an OSL age (84 ± 5.6 ka), that we will discuss below, the site has been assigned to MIS5.

3.2. Valdocarros (VDC) site

Valdocarros is an open-air site located within the CTA in the Jarama valley where the four Arganda units have been recorded. In Arganda I and II units important concentrations of faunal remains and stone tools has been discovered while in the Arganda III there are no remains (Fig. 3). The archaeological excavation was focused in the upper part of the Arganda II (Rubio-Jara et al., 2016). About 840 m² were excavated in 2005 delivering a faunal assemblage of ~2750 bones composed by *Cervus elaphus*, *Equus caballus*, *Dama*, sp., *Elephas* sp., *Bos primigenius*, *Capreolus* sp., *Felis* sp., *Canis lupus* and *Vulpes vulpes*. Bones are very fragmented due to both anthropogenic as well as to fossil diagenetic processes (Yravedra and Domínguez-Rodrigo, 2008). The micromammal assemblage includes Erinaceomorpha: *Erinaceus europaeus*; Soricomorpha: *Crocidura russula*; Rodentia: *Eliomys quercinus*, *Castor fiber*, *Apodemus*

sp., *Cricetulus* (*Allocricetus*) *bursae*, *Arvicola* aff. *sapidus*, *Microtus brecciensis* and Lagomorpha: *Oryctolagus cuniculus* (Sesé et al., 2011b). This places the site of Valdocarros in the Middle Pleistocene, especially by the presence of *Microtus brecciensis*, one of the most characteristic species of this period. The Palaeolithic industry (~3000 stone tools) includes activity of knapping, *façonnage* of handaxes and cores. These stone stools may be ascribed to the Acheulean techno-complex (Panera, 2009; Rubio-Jara et al., 2016).

3.3. Maresa (MA) quarry

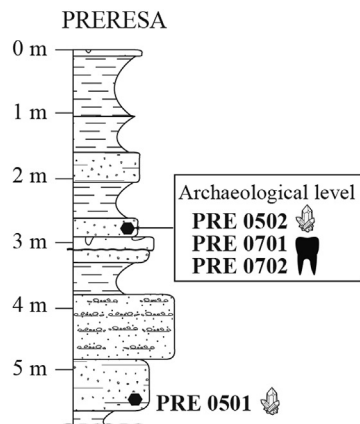
Maresa is a quarry located within the CTA in the Jarama valley where the four Arganda units have also been recorded (Fig. 3). In all of these units, important concentrations of palaeolithic stone tools have been found in secondary position which may be ascribed to the Acheulean techno-complex by correlation with other sites of the region. In the Arganda I unit, an excavation of about 8 m², delivered a partial cervid postcranial skeleton but no micromammal remains or lithic industry associated (Panera, 2009). Palynological analyses suggest the prevailing presence of open landscapes (Ruiz-Zapata et al., 2006). According with two AAR ages (332 ± 38 ka and 379 ± 45 ka), this site could be assigned to Middle Pleistocene.

4. Material and methods

4.1. Sampling

A total of 13 samples (9 samples of sediment and 4 teeth) were collected during three different fieldworks in 2005, 2007 and 2012.

Manzanares valley



Jarama Valley

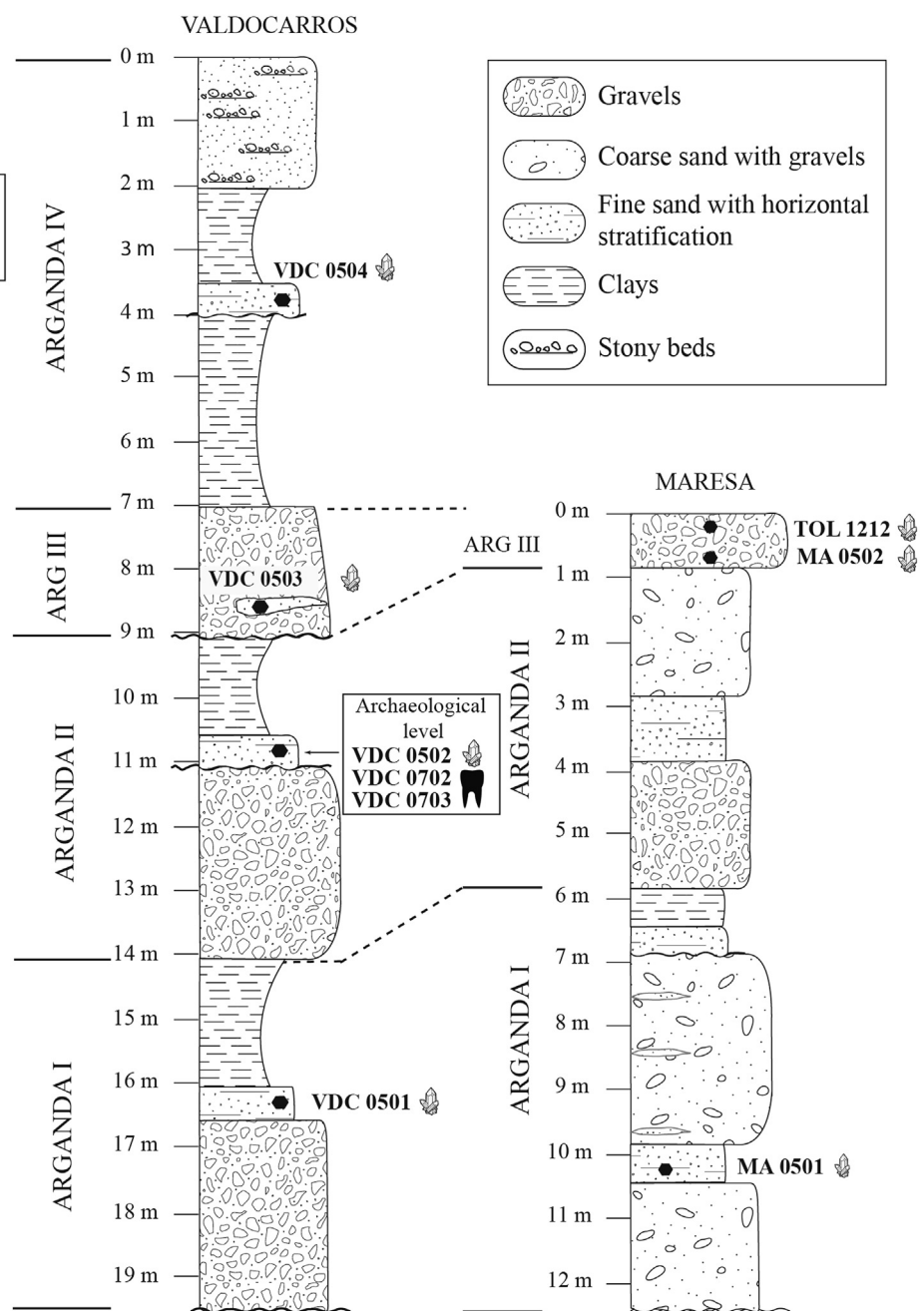


Fig. 3. Local stratigraphy of the sampled sites and position of the ESR samples of quartz ☉ and teeth ☒.

Eight samples of sediment were taken during a fieldwork campaign along the Jarama and Manzanares valleys in 2005 (Figs. 3 and 4). At the Manzanares valley, two samples were collected from the PRERESA site (PRE0501 and PRE0502) which were located about 3 m and 30 cm below the archaeological level, respectively. At the Jarama valley, one sample was collected for each of the Arganda units identified at the Valdocarros site: VDC0501 (Arganda I unit), VDC0502 (Arganda II unit), VDC0503 (Arganda III unit) and VDC0504 (Arganda IV unit). The sample VDC0502 was taken in the archaeological level, whereas VDC0501 was located 5 m below, and VDC0503 and VDC0504 3 and 8 m above the archaeological level, respectively. At the Maresa quarry, two samples were collected:

MA0501 (Arganda I) and MA0502 (Arganda III) respectively 3 m below and 6 m above the archaeological level. At each site, sediment samples were collected from freshly cleaned sections, specifically from sandy levels.

A second fieldwork campaign was carried out in 2007 along the Manzanares and Jarama valleys and four teeth from large mammal were sampled for ESR/U-series analyses. At the Manzanares valley, two teeth were collected from the archaeological level at PRERESA site (PRE0701 and PRE0702). In the Jarama valley, two other teeth were also collected from the archaeological level at Valdocarros site (VDC0702 and VDC0703). *In situ* gamma spectrometry was performed using a NaI probe connected to an Inspector1000

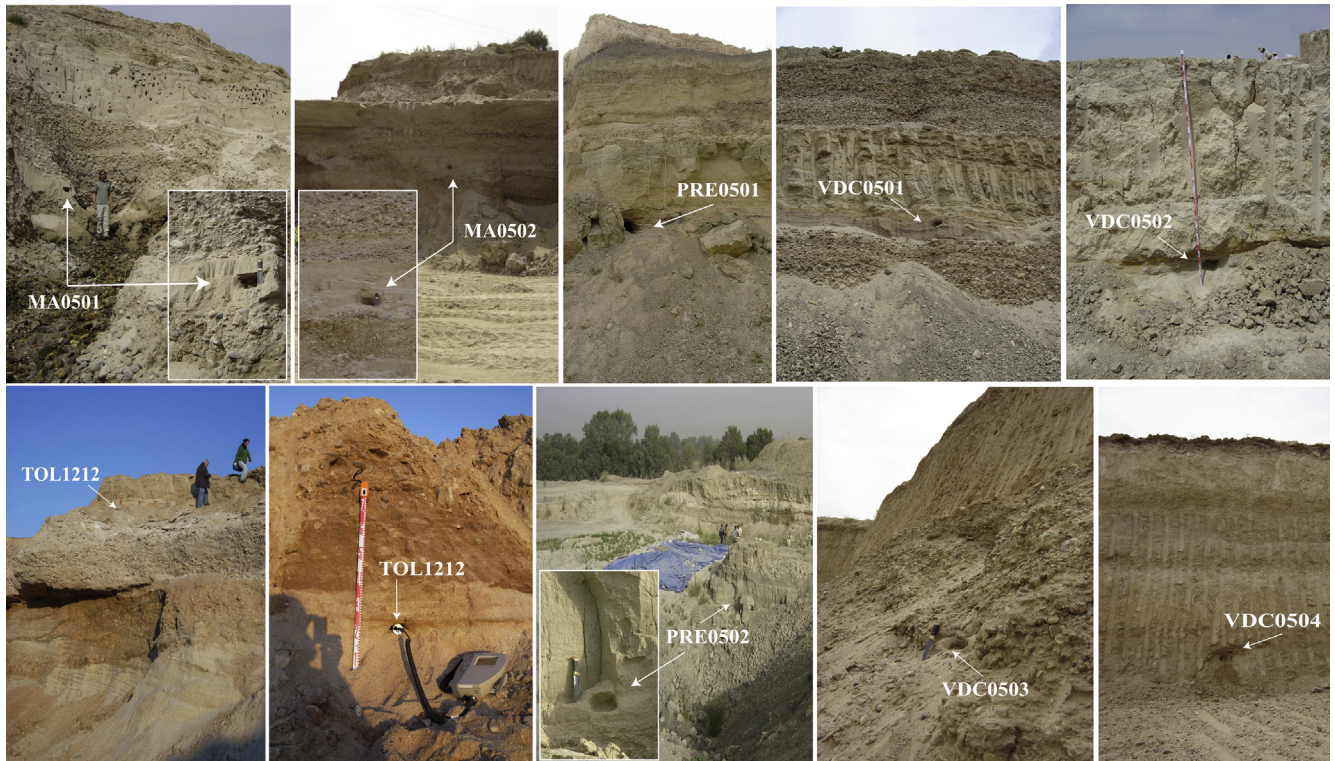


Fig. 4. Pictures of the sections where the nine samples of sediment were collected in Preresá (Manzanares Valley), Maresa and Valdocarros (Jarama Valley) (Photos: M. Duval).

multichannel analyzer (Canberra) and inserted directly into the archaeological layers.

Finally, a third fieldwork campaign occurred in 2012 along the Jarama and Tagus valley and a last sediment sample (TOL1212) was taken in the Arganda III unit at the Maresa quarry. *In situ* gamma spectrometry was performed directly at the exact sampling spot using the same device as previously.

4.2. ESR dating of quartz grains

4.2.1. Sample preparation

Sample preparation was carried out at the Muséum national d'Histoire naturelle (MNHN) (Paris, France) and at the Centro Nacional de Investigación sobre la Evolución Humana (CENIEH) (Burgos, Spain). Sediments were prepared following the standard procedure described in Voinchet et al. (2007) in order to extract pure quartz grains between 100 and 200 μm . The Multiple Aliquots Additive (MAA) dose approach for dating quartz grains was applied. Each sample was divided into 12 multiple grain aliquots. Ten of these aliquots were irradiated using a panoramic ^{60}Co γ -ray source (Dolo et al., 1996) at doses ranging from 400 to 25,000 Gy following a subexponential dose step distribution. During the irradiation, several alanine dosimeters were positioned between the quartz aliquots to monitor the dose effectively received by the samples. For each sample, one aliquot was preserved (natural) and one aliquot was optically bleached for ~1500 h using a SOL2 (Dr. Hönle) solar light simulator in order to evaluate the ESR intensity of the non-bleachable residual signal associated to the Aluminium center of quartz (Voinchet et al., 2003).

4.2.2. ESR dose reconstruction

ESR measurements were performed at low temperature (~90–100 K) using a nitrogen gas flow system connected to a EMX Bruker X-band ESR spectrometer at the Muséum national d'Histoire

naturelle (Paris, France) and an EMXmicro 6/1 Bruker X-band ESR spectrometer at the Centro Nacional de Investigación sobre la Evolución Humana (CENIEH) (Burgos, Spain). The following experimental conditions were employed for the Al center: 5 mW microwave power, 1024 points resolution, 100 kHz modulation frequency, 1 G modulation amplitude, 40 ms conversion time, 40 ms time constant, 9 mT sweep width and 1 scan. The ESR signal associated to the Ti center was measured as follows: 5 mW microwave power, 1024 points resolution, 100 kHz modulation frequency, 1 G modulation amplitude, 60 ms conversion time, 40 ms time constant, 200 G sweep width and 1–3 scan. The angular dependence of the ESR signal due to sample heterogeneity was taken into account by measuring each of the twelve aliquots (one natural, one optically bleached and ten γ -irradiated) of a given sample three times after a ~120° rotation in the cavity. Furthermore, data reproducibility was checked by running ESR measurements over different days. This procedure was carried out for both the Al and Ti signals.

The ESR intensity of Al center was extracted from peak-to-peak amplitude measurements between the top of the first peak ($g = 2.0185$) and the bottom of the 16th peak ($g = 2.002$) of the Al hyperfine structure (Toyoda and Falguères, 2003). The ESR intensity of the Ti centers was measured in four different ways following the conclusions from Duval and Guilarte (2015) (Fig. 5):

- Peak-to-peak amplitude measurement between $g = 1.979$ and the bottom of the peak at $g = 1.913$ (option A; Ti-Li center)
- Peak-to-baseline amplitude measurement around $g = 1.913$ – 1.915 (option D; Ti-Li center)
- Peak-to-baseline amplitude measurement at $g = 1.979$ (Option E; Ti-Li center)
- Peak-to-baseline amplitude measurement around $g = 1.915$ (Option C; Ti-H center).

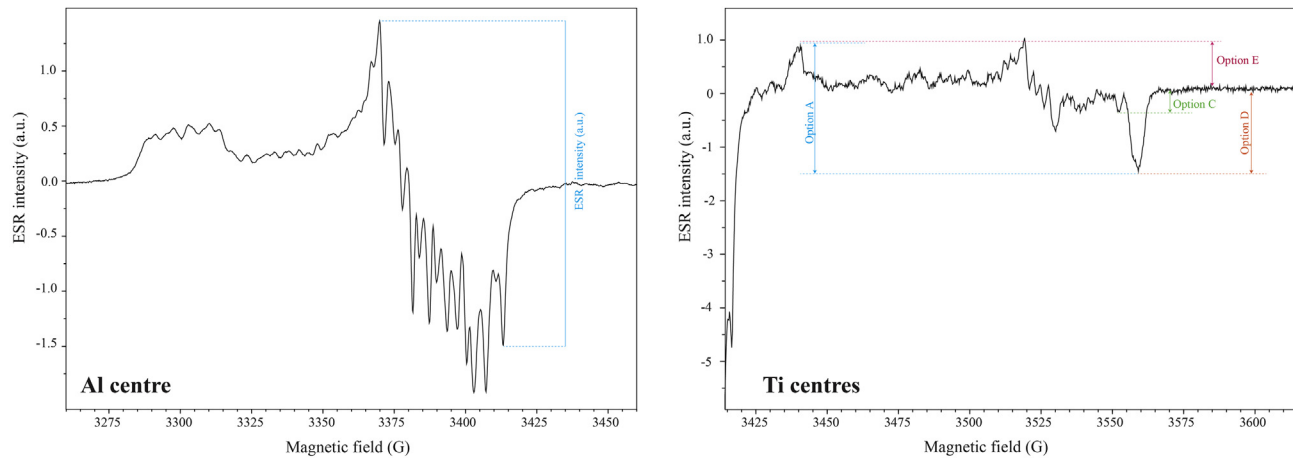


Fig. 5. ESR spectra associated with the Al centre (left) and with the Ti centres (right) measured on a natural aliquot of quartz from Maresa site (TOL1212).

For each aliquot, ESR intensities of Al and Ti centers were corrected by the corresponding receiver gain value, number of scans and aliquot mass. Final ESR intensities correspond to the mean value derived from the repeated measurements.

The equivalent dose (D_E) values were calculated with the Microcal Origin 8.5 software using the Levenberg-Marquardt algorithm by chi-square minimization. For the Al center, a single saturating exponential + linear function (SSE+LIN) (Duval et al., 2009) was fitted through the experimental points. For the Ti centers, two fitting functions were tested (Duval and Guilarte, 2015): the Ti-2 function initially proposed by Woda and Wagner (2007) and the single saturating exponential function (SSE). With the SSE and SSE+LIN functions, data were weighted by the inverse of the squared ESR intensity ($1/I^2$), whereas equal weights were used with the function Ti-2, as described in Duval et al. (2015) (Fig. 6).

4.2.3. Dose rate evaluation and age calculation

The dose rate is derived from the analysis of radioactive elements in the sample and its surroundings.

~5 g of prepared quartz grains were analyzed by ICP-MS analysis in order to obtain the radioelement concentrations (U, Th, K) for the evaluation of the internal dose rate. In addition, ~100 g of raw sediment from all samples were also analyzed by high resolution γ -spectrometry (HRGS) in order to derive α , β and γ external dose rate values (Table 2). For PRE0502 sample, external γ dose rate derived from *in situ* measurements was also available.

Total dose rates were calculated using the dose rate conversion factors from Adamiec and Aitken (1998). Values were corrected

with β and α attenuations for spherical grains (Brennan et al., 1991; Brennan, 2003) and water attenuation formulae from Grün (1994). A water content of 10% was assumed for all samples. A α -efficiency k-value of 0.15 ± 0.10 (Yokoyama et al., 1985) was assumed for the alpha dose rate. The cosmic dose rate was calculated from the equations of Prescott and Hutton (1994), with latitude, altitude and depth corrections.

ESR age calculation was performed using a non-commercial software based on DRAC (Durcan et al., 2015) which takes into account the uncertainties derived from concentrations, depth, water content, *in situ* gamma dose rate, attenuations and D_E values. The errors associated with total doses, equivalent doses and ESR age results are given at 1σ .

4.3. ESR/U-series dating of teeth

Teeth from PRERESA and Valdocarros archaeological levels were analyzed according to the combined ESR/U-series method (Grün et al., 1988).

4.3.1. Sample preparation

Teeth were prepared following the protocol detailed by Bahain et al. (2012) at the MNHN (Paris, France). A part of external enamel layer was extracted from each tooth which was then cleaned on each side in order to avoid any contamination by sediment, cement or dentine. After grounding and sieving, the 100–200 μ m grain-size fraction of the obtained clean enamel was split into 14 aliquots. Thirteen of them were irradiated using ^{60}Co

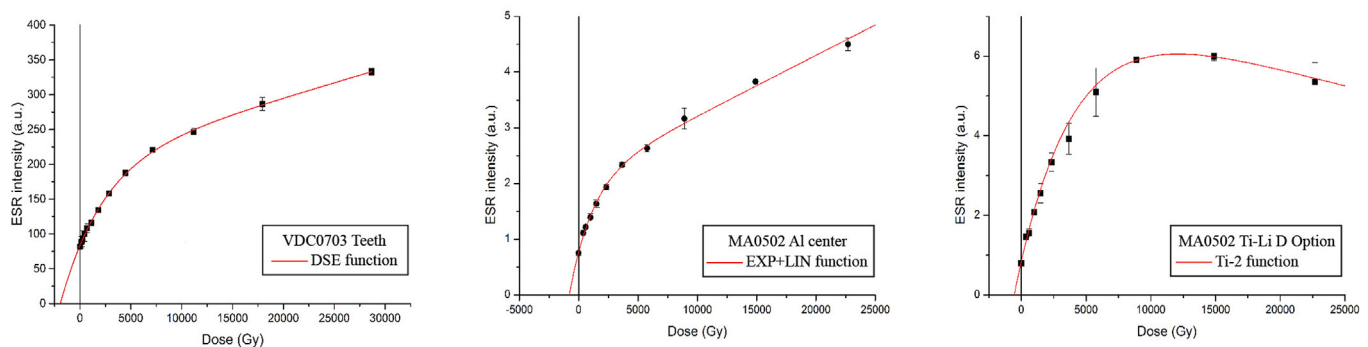


Fig. 6. Examples of three Dose Response Curves obtained in this work. Left: Sample VDC0703, fossil tooth. Middle: Sample MA0502, Al center. Right: Sample MA0502, Ti-Li D option.

Table 2Radioelement concentration values obtained by ICP and high resolution γ spectrometry (HRGS) from powder of raw material and prepared quartz grains.

			Prepared quartz grains			Powder of raw sediment					
			ICP			HRGS			ICP		
			^{238}U (ppm)	^{232}Th (ppm)	^{40}K (%)	^{238}U (ppm)	^{232}Th (ppm)	^{40}K (%)	^{238}U (ppm)	^{232}Th (ppm)	^{40}K (%)
Manzanares valley	PRERESA	PRE0501	0.410 \pm 0.070	1.530 \pm 0.080	3.770 \pm 0.103	4.380 \pm 0.138	18.949 \pm 0.223	4.783 \pm 0.029	0.920 \pm 0.076	3.470 \pm 0.153	3.702 \pm 0.101
		PRE0502	0.430 \pm 0.070	1.460 \pm 0.078	4.210 \pm 0.115	5.202 \pm 0.113	19.930 \pm 0.181	4.194 \pm 0.022			
Jarama valley	Valdocarros	VDC0501	0.340 \pm 0.070	1.130 \pm 0.068	2.090 \pm 0.057	2.188 \pm 0.087	7.222 \pm 0.124	3.502 \pm 0.020			
		VDC0502	0.260 \pm 0.069	0.850 \pm 0.060	2.050 \pm 0.056	1.361 \pm 0.075	4.435 \pm 0.099	3.947 \pm 0.020			
		VDC0503	0.240 \pm 0.069	0.960 \pm 0.063	0.905 \pm 0.025	1.677 \pm 0.093	5.841 \pm 0.136	2.599 \pm 0.021			
		VDC0504	0.300 \pm 0.069	1.310 \pm 0.073	1.590 \pm 0.043	2.565 \pm 0.080	8.904 \pm 0.120	2.283 \pm 0.015			
	Maresa	MA0501	0.110 \pm 0.069	1.310 \pm 0.073	0.246 \pm 0.007	1.678 \pm 0.093	6.134 \pm 0.132	3.115 \pm 0.022			
		MA0502	0.320 \pm 0.069	1.400 \pm 0.076	1.400 \pm 0.038	1.169 \pm 0.095	4.106 \pm 0.124	3.735 \pm 0.026			
		TOL1212	0.350 \pm 0.070	1.530 \pm 0.080	0.107 \pm 0.003						

Table 3Q-ICP-MS U-series data ($\pm 2\sigma$), Rn losses and samples thicknesses ($\pm 1\sigma$) determined on teeth from Preresá (Manzanares valley) and Valdocarros (Jarama valley) sites.

	Manzanares valley				Jarama valley				
	PRERESA				Valdocarros				
	PRE0701		PRE0702		VDC0702		VDC0703		
	Enamel	Dentine	Enamel	Dentine	Enamel	Dentine	Enamel	Dentine	Cement
U content (ppm)	5.319 \pm 0.009	485.09 \pm 9.36	4.90 \pm 0.01	458.08 \pm 8.85	4.45 \pm 0.01	297.96 \pm 1.40	2.82 \pm 0.01	189.83 \pm 1.08	359.47 \pm 3.03
$^{234}\text{U}/^{238}\text{U}$	1.2351 \pm 0.0024	1.2597 \pm 0.0145	1.2825 \pm 0.0027	1.3454 \pm 0.0132	1.1421 \pm 0.0021	1.3907 \pm 0.0048	1.3474 \pm 0.0036	1.3423 \pm 0.0046	1.4317 \pm 0.0046
$^{230}\text{Th}/^{232}\text{Th}$	>100	>100	>100	>100	>100	>100	>100	>100	>100
$^{230}\text{Th}/^{234}\text{U}$	0.7331 \pm 0.0037	0.9546 \pm 0.0285	0.8128 \pm 0.0054	0.8731 \pm 0.0243	0.9928 \pm 0.0047	0.9949 \pm 0.0127	0.9877 \pm 0.0050	1.0187 \pm 0.0080	1.11011 \pm 0.0122
$^{222}\text{Rn}/^{230}\text{Th}$	0.259	0.304	0.996	0.308	0.446	0.329	0.504	0.610	0.285
Initial thickness (μm)	1103 \pm 138		1484 \pm 185		1474 \pm 184		1465 \pm 183		
Removed thickness	39 \pm 5		163 \pm 20		200 \pm 25		154 \pm 19		
Internal side (μm)									
Removed thickness	97 \pm 12		160 \pm 20		183 \pm 23		146 \pm 18		
External side (μm)									

calibrated source (LNHB, CEA, CEN Saclay, France) at doses ranging from to ca. 110–32000 Gy.

4.3.2. ESR dose reconstruction

The ESR intensity of these aliquots and of a remnant natural aliquot were measured at least three times for each dose on different days using a EMX Bruker X-band spectrometer at MNHN (Paris, France) with the following measurement conditions at room temperature: microwave power = 10 mW, modulation amplitude = 0.1 mT, scan range = 10 mT, scan time = 2 min for five scans, frequency modulation = 100 kHz. ESR intensities were derived from peak-to-peak amplitude measurement between T1 and B2 peaks (Grün, 2000). The equivalent doses were then extrapolated from the obtained dose response curve (DRC) using a double saturation exponential function (DSE) (Duval, 2015).

4.3.3. Dose rate evaluation and age calculation

In order to determine the U-uptake parameters necessary to the dose rate contributions and age calculations (Shao et al., 2015), U-series analyses were performed on each dental tissue by Q-ICP-MS (Dauville et al., 2010) following the chemical protocol of Shao et al. (2011): dissolution of 50–150 mg of each sample in 7N HNO₃ and addition of ²³³U, ²³⁶U and ²²⁹Th spike; elution of the solution through an anion exchange resin column (Dowex 1 × 8; 100–200 mesh) in 8N HCl condition allowing thorium to be recovered and uranium to be retained; elution of uranium is performed using 0.1 N HCl; purification of U and Th fractions using respectively a UTEVA resin column in 7 N HNO₃ and a second anion exchange resin column in 7N HNO₃, then elution with 0.1 N HCl for U and 8N HCl for Th; evaporation of the purified U and Th isolates, dissolution of residues in 0.5N HNO₃ and recombination before the ICP-QMS analyses. U-series results are displayed in Table 3. Gamma spectrometry measurements were also made on each dental tissue to evaluate eventual radon losses (Bahain et al., 1992). The beta dose contributions were calculated taking into account a correction linked to the part removed from each side of the enamel layer during the preparation process (according to Brennan et al., 1997) (Table 3).

The radioelement contents of sediment samples associated to the archaeological levels were determined in laboratory by low background high purity gamma spectrometry measurements. The cosmic dose rate was estimated using the formula of Prescott and Hutton (1994). A fixed value of $15 \pm 5\%$ was therefore used for the age calculations. The following parameters were also used: a k-value (α efficiency) of 0.13 ± 0.02 (Grün and Katzenberger-Apel, 1994); water content of 0 wt% in enamels and 7 wt% in dentines and cements; dose rate conversion factors from Adamiec and Aitken (1998). The “US/AU-ESR” computer program (Shao et al., 2012, 2014) was used for the age calculation. This software allows the calculation of ESR/U-series ages with both US (Grün, 2009) and AU (Shao et al., 2012) models, i.e. considering respectively post-mortem U-uptake or both U-Uptake and U-leaching if weak uranium loss are observed. The ESR/U-series data, dose rate contributions and ages are displayed at Table 4.

5. Results

5.1. Combined US-ESR dating of fossil teeth

For PRERESA samples, the tissues of the two analyzed teeth display relatively recent U-uptake allowing the use of US model for PRE0702 tooth and the calculation of a p-parameter for the enamel of PRE0701. The resulting ages for these two teeth are highly consistent, with 206 ± 42 ka and 235 ± 32 ka respectively. In contrast, the Valdocarros teeth show apparent uranium

Table 4
Dose rates and ESR/U-series ages obtained on teeth from Preresá (Manzanares valley) and Valdocarros (Jarama valley) sites. Analytical uncertainties are given with $\pm 1\sigma$.

	Manzanares valley				Jarama valley			
	PRERESA				Valdocarros			
	PRE0701		PRE0702		VDC0702		VDC0703	
	Enamel	Dentine	Enamel	Dentine	Enamel	Dentine	Enamel	Cement
U uptake parameter p or n	-0.6771 ± 0.1755	-0.0070 ± 0.0019	-0.7646 ± 0.0783	-0.8780 ± 0.0622	-0.0045 ± 0.0014	-0.0043 ± 0.0015	-0.0034 ± 0.0006	-0.0035 ± 0.0006
$D_a \alpha$ internal ($\mu\text{Gy/a}$)	840 ± 427		1613 ± 603		885 ± 606		755 ± 250	
$D_a \beta$ ($\mu\text{Gy/a}$)	4020 ± 1883		2610 ± 894		1341 ± 812		3138 ± 753	
$D_a (\gamma + \text{cosm})$ ($\mu\text{Gy/a}$)	2475 ± 50		2475 ± 50		1485 ± 50		1485 ± 50	
D_e (Gy)	1511 ± 252		1574 ± 137		1117 ± 141		1932 ± 145	
D_a total ($\mu\text{Gy/a}$)	7335 ± 1932		6698 ± 1080		3711 ± 1015		5378 ± 795	
ESR/U-series ages US model (ka)	206 ± 42		235 ± 32		301 ± 73		360 ± 46	

Ages results are in bold.

Table 5

Fitting results obtained for Al and Ti centers on quartz grains. The poorness of the Ti-center signal from PRE0501 and VDC0504 samples precluded any reliable and reproducible measurements. The DE values that are not reliable because do not fulfill the criteria defined in Duval (2012) and Duval and Guilarte (2015) for the Al center and Ti center, respectively are given in italics. The DE values used for age calculations are given in bold.

Function			Manzanares valley		Jarama valley						
			PRERESA		Valdocarros						
			PRE0501	PRE0502	VDC0501	VDC0502	VDC0503	VDC0504	MA0501	MA0502	TOL1212
Al center	SSE + LIN	Adj. R ²	0.983	0.985	0.991	0.996	0.991	0.995	0.980	0.995	0.994
		D _E (Gy)	1085 ± 315	1609 ± 328	1366 ± 214	1101 ± 131	2610 ± 446	900 ± 122	782 ± 197	790 ± 83	888 ± 112
Ti-Li center	D Option	Ti2	Adj. R ²	0.985	0.989	0.989	0.922	—	0.947	0.999	0.996
		D _E (Gy)	—	1440 ± 216	1194 ± 269	1233 ± 232	1156 ± 482	—	1492 ± 422	548 ± 63	570 ± 29
	A Option	Ti2	Adj. R ²	—	0.992	0.996	0.985	0.973	—	0.965	0.997
		D _E (Gy)	—	2085 ± 248	1360 ± 99	1120 ± 236	1051 ± 236	—	1283 ± 317	662 ± 68	785 ± 40
	E Option	Ti2	Adj. R ²	—	0.767	0.957	0.956	0.928	—	0.948	0.997
		D _E (Gy)	—	2276 ± 1518	1032 ± 262	904 ± 316	706 ± 315	—	1370 ± 445	550 ± 113	1048 ± 82
Ti-H center	C option	Ti2	Adj. R ²	—	0.834	0.960	0.747	0.211	—	0.746	0.890
		D _E (Gy)	—	436 ± 177	543 ± 208	1207 ± 791	355 ± 508	—	1145 ± 655	212 ± 111	322 ± 53

leaching in all tissues, precluding thus the use of the US model. Consequently, the AU model was systematically used for all the tissues. The AU-ESR ages obtained for the two analysed teeth are highly consistent, with 301 ± 73 ka and 360 ± 46 ka for VDC0702 and VDC0703 respectively.

5.2. ESR dating of optically bleached quartz grains

The ESR analytical data are listed in Tables 2, 5 and 6. All the ESR DRCs derived from the evaluation of the Al, Ti-Li and Ti-H centers are provided in supplementary information (Fig. S1–S5). It should be mentioned here that no reliable ESR data could be obtained from the Ti centers of samples PRE0501 and VDC0504 given the very weak ESR signal.

5.2.1. Fitting results

Regarding the Al center, the dose equivalent (D_E) values were calculated by considering for each aliquot the average ESR intensities obtained from the three repeated measurements carried out over three days. According to Duval (2012), the reliability of the fitting results obtained from the Al center may be reasonably questioned when the adjusted r² value is <0.99 and the relative errors on the fitted parameters >25%. This is the case for some of the samples of the present study, like the two from PRERESA site (PRE0501 and PRE0502, Table 5) in the Manzanares valley. This is contrasting with the fitting results derived from the samples of the Jarama valley (Valdocarros and Maresa) that show adjusted r²

values of 0.99 and the relative D_E errors are ranging from 10% to 17%, with the exception of the sample MA0501.

According to Duval and Guilarte (2015), the D_E obtained from the Ti center should fulfill two criteria in order to confirm their reliability: the adjusted r² value should be greater than 0.98 and the relative errors on the fitted parameters lower than 50%. In our samples, options A and D show adjusted r² values systematically higher than 0.98 indicating a high goodness-of-fit and errors ranging between 7% and 22%, the exception being VDC0503 and MA0501 (options A and D: r² < 0.98 and errors >22%). Options A and D provide overall consistent D_E values for all the samples. The highest differences may be observed for samples PRE0502 and TOL1212, for which option A leads to significantly higher D_E values. This is due to the peak at g = 1.979 which, taken alone (option E), provides much higher D_E values. However, the poor goodness-of-fit observed for most of the samples precludes any further interpretation of those data. Following the work by Duval and Guilarte (2015), final D_E were calculated considering the ESR intensities taken from option D.

Ti-H center (option C) has also been measured and the fitting results are provided in Table 5. This center potentially offers many interests for dating purpose (Duval et al., 2017) but the reliability of the fitting results obtained in the present study may be strongly questioned, given the systematic very poor goodness-of-fit observed (r² ranging between 0.21 and 0.96). Consequently, any further comparison with the results derived from the other centres would therefore result meaningless, and no age calculation was

Table 6

ESR results obtained on quartz grains for the Preressa (Manzanares valley), Valdocarros and Maresa sites (Jarama valley) (Bl: bleaching; D_{int}: internal dose rate; D_α: alpha dose rate; D_β: beta dose rate; D_γ: gamma dose rate; D_{cos}: cosmic dose rate; D_a: total dose rate; D_E: equivalent dose).

	Manzanares valley		Jarama valley				Maresa		
	PRERESA		Valdocarros						
	PRE0501	PRE0502	VDC0501	VDC0502	VDC0503	VDC0504	MA0501	MA0502	TOL1212
Depth (cm)	500	300	1600	1100	850	400	1000	350	110
Bl (%)	51 ± 1	57 ± 6	51 ± 1	54 ± 4	53 ± 2	46 ± 1	55 ± 1	40 ± 3	46 ± 1
D _{int} (μGy/a)	471 ± 24	490 ± 25	330 ± 17	271 ± 14	224 ± 11	311 ± 16	183 ± 9	319 ± 16	169 ± 10
D _α (μGy/a)	139 ± 5	153 ± 6	59 ± 2	37 ± 1	47 ± 2	71 ± 2	48 ± 2	33 ± 1	20 ± 5
D _β (μGy/a)	3956 ± 158	3687 ± 140	2651 ± 114	2792 ± 128	1983 ± 85	1939 ± 76	2323 ± 101	2627 ± 121	2611 ± 71
D _γ (μGy/a)	2271 ± 69	2758 ± 276	1280 ± 42	1175 ± 44	976 ± 32	1126 ± 34	1099 ± 37	1096 ± 42	1020 ± 60
D _{cos} (μGy/a)	89 ± 4	120 ± 6	27 ± 1	42 ± 2	56 ± 3	103 ± 5	47 ± 2	111 ± 6	191 ± 19
D _a (μGy/a)	6926 ± 174	7208 ± 310	4347 ± 123	4317 ± 136	3286 ± 91	3550 ± 84	3700 ± 108	4185 ± 129	4011 ± 96
D _E (Gy) Al	1085 ± 315	1609 ± 328	1366 ± 214	1101 ± 131	2610 ± 446	900 ± 122	782 ± 197	790 ± 83	888 ± 112
D _E (Gy) Ti-Li D option	—	1440 ± 216	1194 ± 269	1233 ± 232	1156 ± 482	—	1492 ± 422	548 ± 63	570 ± 29
Age (ka) Al	157 ± 46	223 ± 47	314 ± 50	255 ± 31	794 ± 138	254 ± 35	211 ± 54	189 ± 21	221 ± 28
Age (ka) Ti-Li D option	—	200 ± 31	275 ± 62	286 ± 54	352 ± 147	—	403 ± 115	131 ± 16	142 ± 8

Ages results are in bold.

carried out for the Ti-H centre.

5.2.2. Internal dose rate

In ESR dating of quartz grains, the internal dose rate is generally assumed to be negligible since quartz is considered free of radioactive elements. However, several studies have shown that this assumption may sometimes be wrong. For example, Sutton and Zimmerman (1978) carried out a few α -activity measurements on quartz extracts which yielded internal dose rates in the range of about 60–200 $\mu\text{Gy/a}$.

In the present study, ICP-MS analysis was systematically performed on the prepared quartz grain samples in order to evaluate their radioelement concentrations (see Table 2). Values obtained for the nine samples range between 0.11 and 0.43 ppm of U and 0.85–1.53 ppm of Th, which result in internal dose rates ranging from 183 ± 9 to 490 ± 25 $\mu\text{Gy/a}$ (Table 6). This is actually an important contribution to the total dose rate (5 to about 7%), which results in a non-negligible impact on the final age results. These high radioelement concentrations may also indicate a possible contamination of the sample by feldspar.

5.2.3. ESR age estimates

5.2.3.1. PRERESA (PRE) site (Manzanares valley). For PRE0501, located on the bottom of the local stratigraphic sequence, only an ESR age (157 ± 46 ka) based on the Al center was obtained because the Ti center could not be measured. The poor reliability of the fitting results may explain the inconsistency of this age with the stratigraphy. In the case of PRE0502 located above, both the Al and Ti centres provide consistent results of 223 ± 47 ka and 200 ± 31 ka, respectively. These ages estimates are in agreement with the ESR results obtained on teeth (206 ± 42 ka and 235 ± 32 ka), suggesting an early MIS 7 chronology (Tables 4 and 6).

5.2.3.2. Valdocarros (VDC) site (Jarama valley). In the Arganda I unit, the two ESR ages obtained for VDC0501 (ESR-Al: 314 ± 50 ka; ESR-Ti: 275 ± 62 ka) are consistent at 1σ , although the ESR-Ti age is younger than the ESR-Al. This might be due to an incomplete bleaching of the signal of the Al center during sediment transport, as the bleaching kinetics of the Ti centers is known to be much faster than that of the Al center (Toyoda et al., 2000). However, this age difference may also be interpreted as being not significant, given the associated errors.

In the Arganda II unit, two ESR ages on optically bleached quartz (VDC0502: 255 ± 31 ka, Al center and 286 ± 54 ka, Ti center) and two ESR/U-series ages (VDC0703: 301 ± 73 and VDC0702: 360 ± 40 ka) have been obtained for the excavation level. Again, both Al and Ti centers provide consistent results at 1σ . These are also in agreement with two out of three AAR ages obtained on ostracods and herbivores molars (254 ± 47 ka; 262 ± 7 ka; 174 ± 20 ka) (Panera et al., 2011). The corresponding ESR/U-series ages on teeth are somewhat older, but nevertheless do not disagree with the other data at 2σ .

For Arganda III unit, the ESR quartz ages estimates for VDC0503 are very scattered, with 794 ± 138 ka (Al center) and 352 ± 147 ka (Ti center). Neither of these ages are consistent with the existing chronology of the terrace sequence at the Jarama valley in which the T14 (+18–20 m; Arganda III unit) has been ascribed to the Upper Pleistocene. Additionally, both Al and Ti center ages seem to be strongly overestimated in comparison with the results obtained for Arganda I and II. This may be explained by the poor fitting results of these samples since in both cases the curve pass over the natural point (see SI). Consequently, we consider that none of these ages may be considered as reliable.

Finally, the sample VDC0504 (Arganda IV unit) has yielded only an ESR quartz age of 254 ± 35 ka based on the D_E value derived from

the Al center. This ESR result is not consistent with both the stratigraphy and the previous chronological data which suggest an age ranging between 112 ± 36 – $22 \pm 74 \pm 5$ ka (Upper Pleistocene, MIS5) (Panera et al., 2005, 2011). An incomplete bleaching of the Al center prior to sediment deposition could explain this over-estimation, but unfortunately the Ti-center age could not be measured to confirm this hypothesis. In any case, the ESR result available should be considered as a maximum possible age for Arganda IV.

5.2.3.3. Maresa (MA) quarry (Jarama valley). The ESR age estimates for the Arganda I unit (MA0501 sample) in Maresa are quite scattered, with 211 ± 54 ka and 403 ± 115 ka for Al and Ti centers, respectively. It is actually quite unusual to observe a Ti age result significantly older than the Al equivalent for a given sample. Because of their placement downstream of the confluence of the Jarama and Manzanares rivers, sediments may be contaminated by older deposits, although it should be mentioned here that the poor goodness-of-fit achieved for both the Al and Ti signals may induce some uncertainty regarding the reliability of the age results obtained. Any further interpretation of those ESR results should be considered with caution.

In Arganda III unit, the ESR ages calculated for the MA0502 (ESR-Al: 189 ± 21 ka; ESR-Ti: 131 ± 16 ka) and for TOL1212 (ESR-Al: 221 ± 28 ka; ESR-Ti: 142 ± 8 ka) samples are consistent within uncertainties. The difference in the Al and Ti ages may be interpreted as an evidence of an incomplete bleaching of the Al center prior to sediment deposition. It is worth pointing out that the sample MA0502 shows an extremely high goodness-of-fit for the Ti-center. The adjusted r^2 values are systematically higher than 0.98 (0.999 for option D, 0.997 for option A and 0.994 for option E) and the D_E values obtained from these three options are all very close (548 ± 63 for option D, 662 ± 68 for option A and 550 ± 113 for option E). Taking into account these data, the ESR-Ti center seems to provide the most likely estimation of the true age of the Arganda III unit at Maresa quarry.

6. Discussion

6.1. Refining the chronology of the PRERESA site (Manzanares valley)

Previous studies pointed out a younger chronology for PRERESA. For example, the small mammal assemblage of PRERESA would be characteristic of the first half of the Upper Pleistocene, mainly due to the presence of *M. cabreræ* (Sesé et al., 2011a), and besides, OSL dating provided an age of 84 ± 5.6 ka (Yravedra et al., 2012). The first records of populations of *Microtus cabreræ* are found at the Middle-Late Pleistocene transition localities of southern France such as Payre (levels F and G) (Desclaux et al., 2008). These levels have TL dates of 232 ± 15 ka and 231 ± 27 ka, respectively and, levels F-G together were dated by Uranium-series to 235 ± 18 ka (Falguères et al., 2008). Nevertheless, recently, the micromammal association of Payre has been related with MIS 6–5 transition (Foury et al., 2016). In the Iberian Peninsula, the first record of this species has been assigned to the Upper Pleistocene. In the Arriaga sand quarry, at the Complex Terrace of Butarque (CTB), the two TL samples which provided minimum ages of 133 ka and 134 ka (Silva et al., 2012) were taken at the same place where *Microtus breccensis* was recorded (Sesé and López-Martínez, 2013), above Arriaga I (Silva et al., 2011). Although others authors attribute those remains to *Microtus cabreræ* (Laplana et al., 2015), the relationship between these ages and Arriaga I should be considered with caution as they were obtained from samples taken more than 30 years after the excavation of the site and it is difficult to correlate

these ages with the micromammal assemblage. On the other hand, the mammal remains at Arriaga IIa above Arriaga I site (*Elephas (P.) antiquus*, *Bos primigenius*, *Equus caballus*, *Cervus elaphus* and *Dicerorhinus hemitoechus*), belong to the typical Middle Pleistocene assemblage of the Madrid region (Sesé and Soto, 2000).

If the attribution and the chronology for Arriaga I are confirmed, it would be in agreement with the PRERESA site, and so the outcrop Complex Terrace of Butarque, may be somewhat older than previously expected, belonging to the end of the Middle Pleistocene. Taking into account that *Microtus brecciensis* is the direct ancestor of *Microtus cabreræ* (Cabrera-Millet et al., 1982), which gradually reduced its distribution range from the late Pleistocene to the present (López-Martínez, 2009), and that at Mollet there is an isochron age for Layer 5 with *Microtus brecciensis* of 215 ka, provided by uranium-series method (Maroto et al., 2012; López-García et al., 2014), the most likely chronology for PRERESA site is the youngest age of its range (169–270 ka). It would therefore be the beginning of MIS 6.

Consequently, the chronological distribution of *Microtus cabreræ* would more likely cover from the late Middle Pleistocene to the Holocene, making PRERESA site (Manzanares valley) the oldest record of this species in the Iberian Peninsula (Fig. 7).

6.2. Geomorphological interpretation of the ESR age results at the Jarama valley

As described in section 2.2, the Arganda Complex Terrace (TCA), located in the low valley of Jarama river and where the Valdocarros (VDC) and Maresa (MA) sites were discovered, is formed by successive alluvial deposits identified as Arganda I, II, III and IV, from bottom to top. One of the main aims of this work was to improve the current chronostratigraphic framework of these alluvial deposits (Arganda units) (Fig. 8).

Taking into account the ESR ages obtained in the present work for Arganda I at Valdocarros site (VDC0501: 314 ± 50 ka and 275 ± 62 ka) and the previous Amino Acid Racemization ages (AAR) obtained at Maresa site (332 ± 38 ka and 379 ± 45 ka) (Panera et al., 2011) an age ranging between 295 and 365 ka (MIS10-9) may be the most likely estimation of the true age for this unit. The limits of this age range have been located where there is a greater number of age overlap (Fig. 8). The ESR ages estimates for this unit at Maresa quarry (MA0501: 211 ± 54 ka and 403 ± 115 ka) have not been taking into account because of their poor reliability. Proceeding as in the Arganda I and using the ESR ages on quartz (ESR-Al: 255 ± 31 ka; ESR-Ti-Li: 286 ± 54 ka) and the ESR ages on teeth (360 ± 46 ka

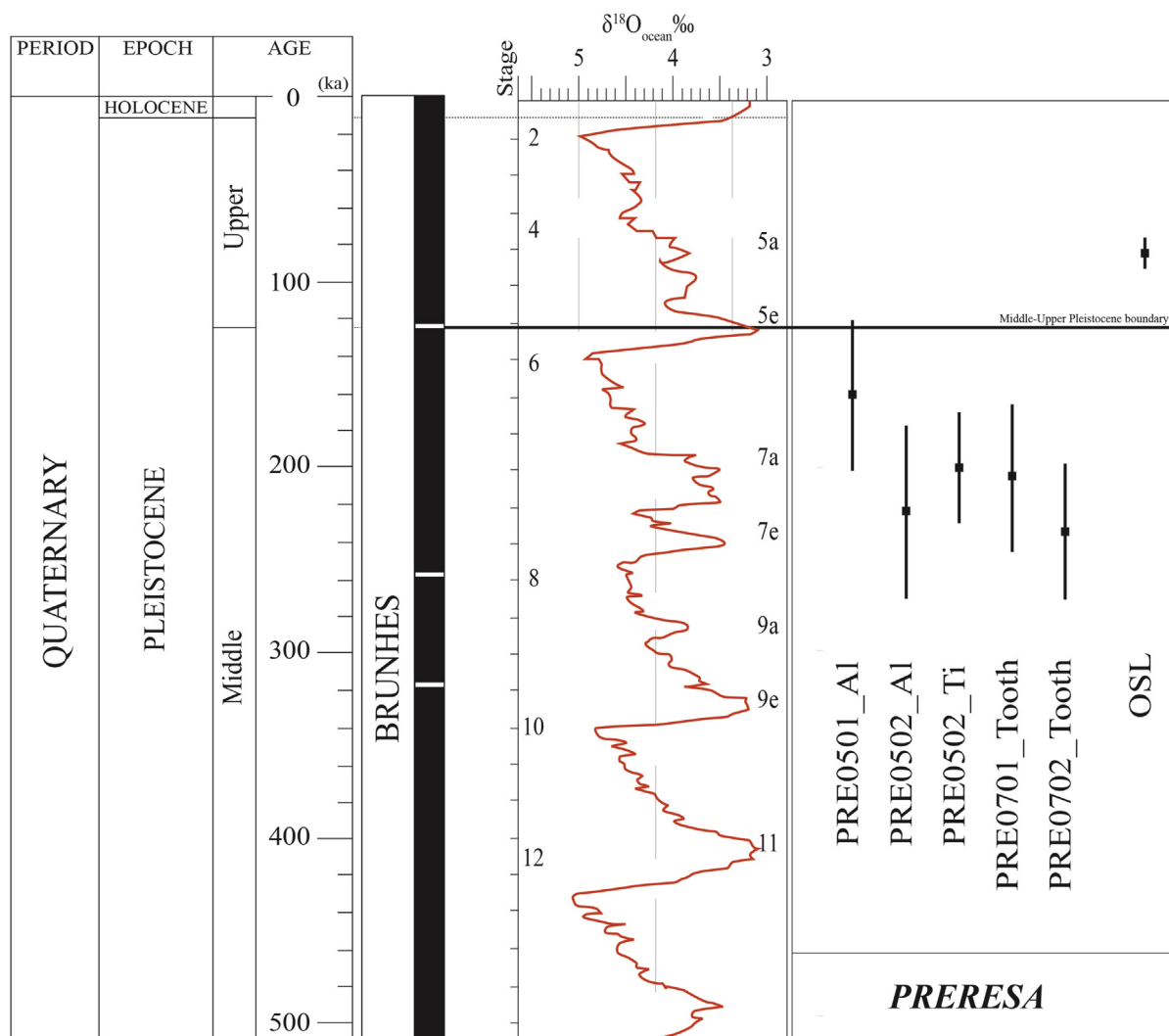


Fig. 7. Geochronological framework suggested for the PRERESA site (Complex Terrace of Butarque, CTB, Manzanares valley) on the basis of the published ages obtained by OSL (Yravedra et al., 2012; Panera et al., 2014) and the ESR ages obtained in the present work.

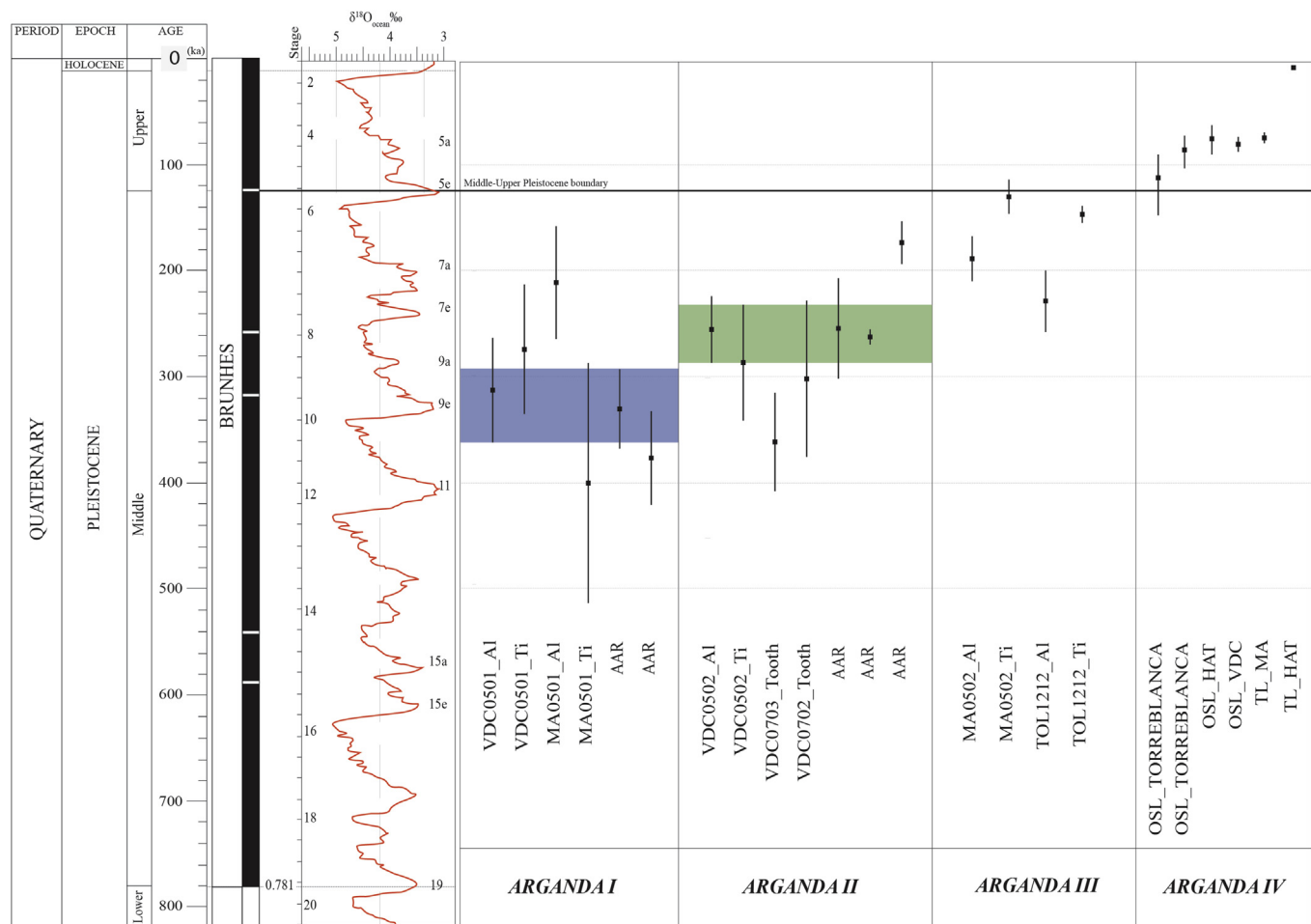


Fig. 8. Geochronological framework suggested for the Arganda I, II, III and IV units (Arganda Complex Terrace, TCA, Jarama valley) on the basis of the published ages obtained by TL, OSL and AAR (Panera et al., 2011) and the ESR ages obtained in the present work.

and 301 ± 73 ka) obtained in this work and the previous AAR ages (254 ± 47 ka, 262 ± 07 ka and 174 ± 20 ka) at Valdocarros site (Panera et al., 2011), an age range between 235 and 285 ka (MIS8) could be given for the Arganda II unit. In the Arganda III unit, only the ESR ages on quartz obtained at Maresa quarry: MA0502 (Al: 189 ± 21 ka and Ti-Li: 131 ± 16 ka) and TOL1212 (Al: 228 ± 29 ka and Ti-Li: 146 ± 8 ka) can be used because of the inconsistency of the results derived from the sample VDC0503 at Valdocarros site. In that regard, the difference in the Al and Ti ages for these samples has been interpreted as an evidence of an incomplete bleaching of the Al. Therefore, the ESR-Al ages of 228 ± 29 ka and 189 ± 21 ka should be considered as maximum possible age estimates for this unit while the ESR ages derived from the Ti center (146 ± 8 ka and 131 ± 16 ka) would provide the more correct estimation of the true age suggesting that the Arganda III unit was deposited during the MIS6. Finally, the ESR data provided by the sample VDC0504 at Valdocarros site is inconsistent with stratigraphy and paleontological data available. The age of the Arganda IV unit is therefore given by the previous chronological data obtained by OSL and TL at different localities (HAT, Torreblanca, Maresa y Valdocarros) (Panera et al., 2005, 2011) which suggest a clear chronological position to the Arganda IV to the Upper Pleistocene (MIS5). This unit Arganda IV is a slope deposit which transportation process is not favorable for ESR dating.

7. Conclusion

This study presents several ESR ages (quartz and teeth) for three archaeological sites located on the fluvial deposits of the Manzanares River (PRERESA site) and the Jarama River (Valdocarros site and Maresa quarry) to the southeast of Madrid (Central Spain). The ESR dating study presented in this work suggests that the PRERESA site (Manzanares valley) may be somewhat older than previously expected, belonging to the end of the Middle Pleistocene (early MIS6). The numerical ages obtained at the Jarama valley show good consistency with previous chronological data, stratigraphy and micro-mammals for the Arganda I, II and III units. Consequently, based on the results obtained in the present work, Arganda I unit may be chronologically positioned between MIS10 and MIS9, Arganda II unit between MIS8 and MIS7 and Arganda III close to the MIS6. In contrast, the results obtained for Arganda IV are inconsistent with both stratigraphy and previous numerical ages. To complete those ESR results, more samples should be taken in the future, especially for the upper Arganda alluvial units (Arganda III and IV).

To conclude, the present work contributes to refine the chronology of three important Palaeolithic sites and to reinforce the chronological framework of two of the most important tributaries rivers of the Tagus River. The age scattering observed in the Arganda III and IV demonstrates the necessity to take more than

one sample to get a reliable estimate of the chronology of a given archaeological site or deposit. These ESR dating study shows the interest of using ESR dating of optically bleached quartz grains extracted from fluvial sediments in order to calculate numerical ages for the whole Middle Pleistocene, as well as the importance of measuring both the Al- and Ti-centers in a given sample.

Acknowledgments

This research has been funded by the Dirección General de Patrimonio Histórico (PR170/04-13244; PR42/05-14071; 1962/2006/00) and the Dirección General de Investigación of the Comunidad de Madrid (06/123/2003). The authors wish to thank T. Garcia and J.M. Dolo (Commissariat à l'Energie Atomique, Paris, France) for the alanine irradiation and V. Guilarte for her support in the preparation of one of the samples. Financial support was provided to the Department of Prehistory of the Muséum National d'Histoire Naturelle by the Conseil Régional d'Ile-de-France for the acquisition of an ESR EMX Bruker spectrometer and by the Ministère de la Culture, sous-direction de l'Archéologie, Service Régional de l'Archéologie of the Region Centre (France) for the acquisition of a portable γ -spectrometer. M. Duval is currently the recipient of an Australian Research Council Future Fellowship (FT150100215).

Appendix A. Supplementary data

Supplementary data related to this article can be found at <http://dx.doi.org/10.1016/j.quaint.2017.09.003>.

References

- Adamiec, G., Aitken, M.J., 1998. Dose-rate conversion factors: update. *Anc. TL* 16, 37–50.
- Bahain, J.J., Yokoyama, Y., Falguères, C., Sarcia, M.N., 1992. ESR dating of tooth enamel: a comparison with K-Ar dating. *Quat. Sci. Rev.* 11, 245–250.
- Bahain, J.J., Falguères, C., Laurent, M., 2012. ESR and ESR/U-series dating study of several middle Palaeolithic sites of Pléneuf-Val-André (Brittany, France): Piégu, Les Vallées and Nantois. *Quat. Geochronol.* 10, 424–429.
- Benito, G., Gutiérrez, F., Pérez-González, A., Machado, M.J., 2000. Geomorphological and sedimentological features in Quaternary fluvial systems affected by solution-induced subsistence (Ebro basin, NE Spain). *Geomorphology* 33, 206–224.
- Benito-Calvo, A., Pérez-González, A., Parés, J.M., 2008. Quantitative reconstruction of Late Cenozoic landscapes: a case study in the Sierra de Atapuerca (Burgos, Spain). *Earth Surf. Process. Landforms* 33, 196–208.
- Blain, H.A., Panera, J., Uribealrrea, D., Rubio-Jara, S., Pérez-González, A., 2012. Characterization of a rapid climate shift at the MIS 8/7 transition in central Spain (Valdocarros II, Autonomous Region of Madrid) by means of the herpetological assemblages. *Quat. Sci. Rev.* 47, 73–81.
- Blain, H.A., Sesé, C., Rubio-Jara, S., Panera, J., Uribealrrea, D., Pérez-González, A., 2013. Reconstruction paléoenvironnementale et paléoclimatique du Pléistocène supérieur ancien (MIS 5a) dans le centre de l'Espagne: les petits vertébrés (Amphibia, Reptilia & Mammalia) des gisements de HAT et PRERESA (Sud-est de Madrid). *Quaternaire* 24 (2), 191–205.
- Brennan, B.J., 2003. Beta doses to spherical grains. *Radiat. Meas.* 37 (4–5), 299–303.
- Brennan, B.J., Lyons, R.G., Phillips, S.W., 1991. Attenuation of alpha particle track dose for spherical grains. *Int. J. Radiat. Appl. Instrum. Part D. Nucl. Tracks Radiat. Meas.* 18, 249–253.
- Brennan, B.J., Rink, W.J., McGuire, E.L., Schwarcz, H.P., Prestwich, W.V., 1997. Beta doses in tooth enamel by “one-group” theory and the ROSY ESR dating software. *Radiat. Meas.* 27, 307–314.
- Cabrera-Millet, M., Britton-Davidian, J., Orsini, P., 1982. Génétique biochimique comparée de *Microtus cabrerai* Thomas, 1906 et de trois autres espèces d'Arvicolidae méditerranéens. *Mammalia* 46 (3), 381–388.
- De Vicente, G., Muñoz-Martín, A., 2013. The Madrid Basin and the Central System: a tectonostratigraphic analysis from 2D seismic lines. *Tectonophysics* 602, 259–285.
- De Vicente, G., González-Casado, J.M., Muñoz-Martín, A., Giner, J., Rodríguez-Pascua, M.A., 1996. Structure and tertiary evolution of the Madrid basin. In: Frien, P.F., Dabrio, C.J. (Eds.), *Tertiary Basins of Spain: the Stratigraphic Record of Crustal Kinematics*. University Press, Cambridge, pp. 263–267.
- Desclaux, E., El Hazzazi, N., Villette, P., Dubar, M., 2008. Le contexte environnemental des occupations humaines. L'apport de la microfaune, des restes aviaires et de la malacofaune. In: Moncel, M.H. (Ed.), *Le site de Payre: Occupations Humaines dans la vallée du Rhône à la fin du Pléistocène Moyen et au début du Pléistocène supérieur*, Mémoires de la Société Préhistorique Française, vol. 46, pp. 91–105.
- Dolo, J.M., Lecerf, N., Mihajlovic, V., Falguères, C., Bahain, J.J., 1996. Contribution of ESR dosimetry for irradiation of geological and archaeological samples with a ^{60}Co panoramic source. *Appl. Radiat. Isotopes* 47, 1419–1421.
- Domínguez-Alonso, R.M., Arcos Fernández, S., Ruiz Zapata, B., Gil García, M.J., 2009. Nuevos datos sobre la Terraza compleja de Butarque en Villaverde Bajo. In: *Actas de las IV Jornadas de Patrimonio Arqueológico de la Comunidad de Madrid* (2007), CARM, Madrid, pp. 339–343.
- Douville, E., Sallé, E., Frank, N., Eisele, M., Pons-Branchu, E., Ayrault, S., 2010. Rapid and accurate U-Th dating of ancient carbonates using inductively coupled plasma-quadrupole mass spectrometry. *Chem. Geol.* 272, 1–11.
- Durcan, J.A., King, G.E., Duller, G.A.T., 2015. DRAC: dose rate and age calculator for trapped charge dating. *Quat. Geochronol.* 28, 54–61.
- Duval, M., 2012. Dose response curve of the ESR signal of Aluminium center in quartz grains extracted from sediment. *Anc. TL* 30 (2), 41–49.
- Duval, M., 2015. Evaluating the accuracy of ESR dose determination of pseudo-Early Pleistocene fossil tooth enamel samples using dose recovery tests. *Radiat. Meas.* 79 (0), 24–32.
- Duval, M., Guilarte, V., 2015. ESR dosimetry of optically bleached quartz grains extracted from Plio-quaternary sediment: evaluating some key aspects of the ESR signals associated to the Ti-centers. *Radiat. Meas.* 78, 28–41.
- Duval, M., Grün, R., Falguères, C., Bahain, J.J., Dolo, J.M., 2009. ESR dating of Lower Pleistocene fossil teeth: Limits of the single saturating exponential (SSE) function for the equivalent dose determination. *Radiat. Meas.* 44, 477–482.
- Duval, M., Sancho, C., Calle, M., Guilarte, V., Peña-Monné, J.L., 2015. On the interest of using the multiple centers approach in ESR dating of optically bleached quartz grains: some examples from the Early Pleistocene terraces of the Alcanadre River (Ebro basin, Spain). *Quat. Geochronol.* 29, 58–69.
- Duval, M., Arnold, L.J., Guilarte, V., Demuro, M., Santonja, M., Pérez-González, A., 2017. Electron Spin Resonance dating of optically bleached quartz grains from the Middle Palaeolithic site of Cuesta de la Bajada (Spain) using the multiple centres approach. *Quat. Geochronol.* 37, 82–96.
- Falguères, C., Bahain, J.J., Masaoudi, H., 2008. Datation de restes paléontologiques par combinaison des méthodes de la résonance de spin électronique et des séries de l'uranium (méthode ESR/U-Th combinée). In: Moncel, M.H. (Ed.), *Le site de Payre: Occupations Humaines dans la vallée du Rhône à la fin du Pléistocène Moyen et au début du Pléistocène supérieur*, Mémoires de la Société Préhistorique Française, vol. 46, pp. 110–112.
- Foury, Y., Desclaux, E., Daujeard, C., Defleur, A., Moncel, M.H., Raynal, J.P., 2016. Évolution des faunes de rongeurs en moyenne vallée du Rhône (Rive droite, Ardèche, France) au cours du Pléistocène Moyen final et du Pléistocène Supérieur ancien, du MIS6 au MIS4. *Quaternaire* 27 (1), 55–79.
- Giner, J.L., De Vicente, G., Pérez-González, A., Sánchez Cabañero, J.G., Pinilla, L., 1996. Crisis tectónicas cuaternarias en la Cuenca de Madrid. *Geogaceta* 20 (4), 842–845.
- Goy, J.L., Pérez-González, A., Zazo, C., 1989. Cartografía y Memoria del Cuaternario, Hoja 19-22 (Madrid). In: *Mapa Geológico de España 1:50.000 MAGNA*. Servicio de Publicaciones del Ministerio de Industria, Madrid, p. 79.
- Grün, R., 1994. A cautionary note: use of the water content and depth for cosmic ray dose rate in AGE and DATA programs. *Anc. TL* 12, 50–51.
- Grün, R., 2000. Methods of dose determination using ESR spectra of tooth enamel. *Radiat. Meas.* 32 (5–6), 767–772.
- Grün, R., 2009. The DATA program for the calculation of ESR age estimates on tooth enamel. *Quat. Geochronol.* 4, 231–232.
- Grün, R., Katzenberger-Apel, O., 1994. An alpha irradiator for ESR dating. *Anc. TL* 12, 35–38.
- Grün, R., Schwarcz, H.P., Chadam, J., 1988. ESR dating of tooth enamel: coupled correction for U-uptake and U-series disequilibrium. *Nucl. Tracks. Radiat. Meas.* 14, 237–241.
- Laplana, C., Herráez, E., Yravedra Sáinz de los Terreros, J., Báez, S., Rubio-Jara, S., Panera, J., Rus, I., Pérez-González, A., 2015. Biocronología de la Terraza Compleja de Butarque del río Manzanares en el Estanque de Tormentas al sur de Madrid (España). *Estud. Geol.* 71 (1), 1–16.
- López-García, J.M., Blain, H.A., Julià, R., Maroto, J., 2014. Environment and climate during MIS7 and their implications for the late Middle Pleistocene hominins: the contribution of Mollet cave, Serinyà, Girona, northeastern Iberian Peninsula. *Quat. Int.* 337, 4–10.
- López-Martínez, N., 1980. Los micromamíferos (Rodentia, Insectivora, Lagomorpha Chiroptera), del sitio de ocupación Achelense de Áridos 1-1 (Arganda, Madrid). In: Santonja, M., López Martínez, N., Pérez-González, A. (Eds.), *Occupaciones Achelenses en el valle del Jarama* (Arganda, Madrid), Arqueología y Paleoeología, vol. 1. Diputación Provincial de Madrid, pp. 161–202.
- López-Martínez, N., 2009. Time asymmetry in the palaeobiogeographic history of species. *Bull. la Soc. Géol. Fr.* 180, 45–55.
- Manzano, L., Expósito, A., Pérez-González, A., Soto, E., Sesé, C., Yravedra, J., Ruiz-Zapata, B., Millán, A., Benítez, P., Torres, T., Mondéjar, J.A., Zarco, E., Sánchez, H., Citores, A., Ramos, M., Rodríguez, A., 2010. El yacimiento arqueológico paleontológico de E.D.A.R.CULEBRO 1 (Estación Depuradora de Aguas Residuales de la cuenca Baja del Arroyo Culebro). In: *Ministerio de Medio Ambiente. Confederación Hidrográfica del Tajo. Actas de las V Jornadas de Patrimonio Arqueológico en la Comunidad de Madrid celebradas en el Museo Arqueológico Regional de la Comunidad de Madrid del 12-14 noviembre de 2008*. Alcalá de Henares, Madrid, pp. 203–214.
- Maroto, J., Julià, R., López-García, J.M., Blain, H.A., 2012. Chronological and

- environmental context of the middle Pleistocene human tooth of mollet cave (Serinyà, NE Iberian Peninsula). *J. Hum. Evol.* 62, 655–663.
- Moreno, D., Falguères, C., Pérez-González, A., Duval, M., Voinchet, P., Benito-Calvo, A., Ortega, A.L., Bahain, J.J., Sala, R., Carbonell, E., Bermúdez de Castro, J.M., Arsuaga, J.L., 2012. ESR chronology of alluvial deposits in the Arlanzón valley (Atapuerca, Spain): contemporaneity with Atapuerca Gran Dolina site. *Quat. Geochronol.* 10, 418–423.
- Panera, J., 2009. La ocupación del medio fluvial en el Paleolítico antiguo. Caracterización geoarqueológica de depósitos pleistocenos del valle del río Jarama (Madrid) y estudio tecnoeconómico de la industria lítica. Tesis Doctoral. Departamento de Prehistoria y Arqueología. Facultad de Geografía e Historia. Universidad Nacional de Educación a Distancia. Inédita, 705 pp.
- Panera, J., Rubio-Jara, S., 2002. Bifaces y elefantes. La investigación del Paleolítico Inferior en Madrid. In: *Zona Arqueológica*, vol. 1, p. 510.
- Panera, J., Pérez-González, A., Rubio-Jara, S., Sesé, C., 2005. El yacimiento paleolítico de HAT en el valle del Jarama: una aportación de Cuaternario de la cuenca de Madrid al debate sobre el inicio del Paleolítico medio. In: Santonja, M., Pérez-González, A., Machado, M.J. (Eds.), *Geoarqueología y Patrimonio en la Península Ibérica y el entorno Mediterráneo*. ADEMA, pp. 251–260.
- Panera, J., Torres, T., Pérez-González, A., Ortiz, J.E., Rubio-Jara, S., Uribelarrea del Val, D., 2011. Geocronología de la Terraza Compleja de Arganda en el valle del río Jarama (Madrid, España). *Estud. Geol.* 67 (2), 495–504.
- Panera, J., Rubio-Jara, S., Yravedra, J., Blain, H.A., Sesé, C., Pérez-González, A., 2014. Manzanares valley (Madrid, Spain): a good country for Proboscideans and Neanderthals. *Quat. Int.* 326–327, 329–343.
- Pérez-González, A., 1971. Estudio de los procesos de hundimiento en el valle del río Jarama y sus terrazas (notas preliminar). *Estud. Geol.* 27 (4), 317–324.
- Pérez-González, A., 1980. El marco geográfico, geológico y geomorfológico de los yacimientos de Áridos en la Cuenca del Tajo. In: Santonja, M., López, N., Pérez-González, A. (Eds.), *Ocupaciones achelenses en el valle del Jarama (Arganda, Madrid)*. Arqueología y Paleontología, vol. 1. Diputación Provincial de Madrid, pp. 15–28.
- Pérez-González, A., 1994. Depresión del Tajo. In: Gutiérrez Elorza, M. (Ed.), *Geomorfología de España*. Ed. Rueda, Madrid, pp. 389–436.
- Pérez-González, A., Uribelarrea, D., 2002. Geología del cuaternario en los valles fluviales del Jarama y Manzanares en las proximidades de Madrid. *Zona Arqueol.* 1, 302–317.
- Pérez-González, A., Rubio-Jara, S., Panera, J., Uribelarrea, D., 2008. Geocronología de la sucesión arqueostratigráfica de Los Estragales en la Terraza Compleja de Butarque (Valle del río Manzanares, Madrid). *Geogaceta* 45, 39–42.
- Pérez-González, A., Gallardo-Millán, J.L., Uribelarrea del Val, D., Panera, J., Rubio-Jara, S., 2013. La inversión Matuyama-Brunhes en la secuencia de terrazas del río Jarama entre Velilla de San Antonio y Altos de la Mejorada, al SE de Madrid (España). *Estud. Geol.* 69 (1), 35–46.
- Prado, C. de, 1864. Descripción física y geográfica de la Provincia de Madrid, 2ª ed. Junta General de Estadística, Madrid, 1975. (Colegio de Ingenieros de Caminos, Canales y Puertos, Madrid).
- Prescott, J.R., Hutton, J.T., 1994. Cosmic ray contributions to dose rates for luminescence and ESR dating: large depths and long-term time variations. *Radiat. Meas.* 23, 497–500.
- Rubio-Jara, S., 2011. El paleolítico en el valle del río Manzanares (Madrid). Caracterización geoarqueológica de depósitos pleistocenos y estudio tecnoeconómico de la industria lítica (Unpublished PhD thesis). Universidad Nacional de Educación a Distancia (UNED).
- Rubio-Jara, S., Panera, J., Santonja, M., Pérez-González, A., 2002. Revisión crítica y síntesis del Paleolítico de los valles del Manzanares y Jarama. In: Panera, J., Rubio-Jara, S. (Eds.), *Bifaces y elefantes. La investigación del Paleolítico inferior en Madrid*. Zona Arqueológica, vol. 1. Museo Arqueológico Regional, Alcalá de Henares, Spain, pp. 338–355.
- Rubio-Jara, S., Panera, J., Rodríguez-de-Tembleque, J., Santonja, M., Pérez-González, A., 2016. Large flake Acheulean in the middle of Tagus basin (Spain): middle stretch of the river Tagus valley and lower stretches of the rivers Jarama and Manzanares valleys. *Quat. Int.* 411, 349–366.
- Ruiz-Zapata, B., Pérez-González, A., Panera, J., Dorado, M., Valdeolmillos, A., Gómez, C., Gil García, M.J., 2006. Middle Pleistocene vegetation in the valley of Jarama river (Casa de la Peña site, Arganda del Rey, Madrid, Spain). In: 7th European Palaeobotany-palynology Conference. Prague, 2006.
- Santonja, M., López, N., Pérez-González, A. (Eds.), 1980. *Ocupaciones achelenses en el valle del Jarama*. Arqueología y Paleontología, vol. 1. Diputación Provincial de Madrid, Madrid.
- Sesé, C., Soto, E., 2000. Vertebrados del Pleistoceno de Madrid. In: Morales, J. (Ed.), *Patrimonio Paleontológico de la comunidad de Madrid*. Arqueología, Paleontología y Etnografía, vol. 6. Comunidad de Madrid, Madrid, pp. 216–243.
- Sesé, C., López-Martínez, N., 2013. Nuevos datos paleontológicos del Pleistoceno en el Valle del Manzanares (Madrid, España): Los micromamíferos del yacimiento del Arenero de Arriaga. *Estud. Geol.* 69 (2), 271–282.
- Sesé, C., Rubio-Jara, S., Panera, J., Pérez-González, A., 2011a. Micromamíferos del Pleistoceno Superior del yacimiento de PRERESA en el valle del Manzanares y su contribución a la reconstrucción paleoambiental de la cuenca de Madrid durante el Pleistoceno. *Estud. Geol.* 67 (2), 471–494.
- Sesé, C., Rubio-Jara, S., Panera, J., Pérez-González, A., 2011b. Micromamíferos del Pleistoceno Medio y Superior en el valle del Jarama: yacimientos de Valdocarros y HAT (Madrid, España). *Estud. Geol.* 67 (1), 131–151.
- Shao, Q., Bahain, J.J., Falguères, C., Peretto, C., Arzarello, M., Minelli, A., Hohenstein, U.T., Dolo, J.M., Garcia, T., Frank, N., Douville, E., 2011. New ESR/U-series data for the early middle Pleistocene site of Isernia la Pineta, Italy. *Radiat. Meas.* 46, 847–852.
- Shao, Q., Bahain, J.J., Falguères, C., Dolo, J.M., 2012. A new U-uptake model for combined ESR/U-series dating of tooth enamel. *Quat. Geochronol.* 10, 406–411.
- Shao, Q., Bahain, J.J., Dolo, J.M., Falguères, C., 2014. Monte Carlo approach to calculate US-ESR age and age uncertainty for tooth enamel. *Quat. Geochronol.* 22, 99–106.
- Shao, Q., Chadam, J., Grün, R., Falguères, C., Dolo, J.M., Bahain, J.J., 2015. The mathematical basis for the US-ESR dating method. *Quat. Geochronol.* 30, 1–8.
- Silva, P.G., 2003. El Cuaternario del valle inferior del Manzanares (Cuenca de Madrid, España). *Estud. Geol.* 59, 107–131.
- Silva, P., Goy, J.L., Zazo, C., 1988. Neotectónica del sector centro-meridional de la cuenca de Madrid. *Estud. Geol.* 44, 415–427.
- Silva, P.G., López-Recio, M., González Hernández, F.M., Tapias, F., Alarcón, A., Cuartero, F., Expósito, A., Lázaro, I., Manzano, I., Martín, D., Morín, J., Yravedra, J., 2008. Datos geoarqueológicos de la terraza compleja del Manzanares entre el sector del 12 de Octubre y la desembocadura del arroyo Butarque (Villaverde, Madrid). *Cuaternario Geomorfol.* 22, 47–70.
- Silva, P.G., Tapias, F., López-Recio, M., Carrasco, P., Morín, J., Roquero, E., Rus, I., 2011. Análisis estratigráfico del arenero de Arriaga (Terraza compleja del Manzanares, Madrid). In: *Resúmenes XIII Reunión Nacional de Cuaternario*. Andorra 2011.
- Silva, P.G., López-Recio, M., Cuartero, F., Baena, J., Tapias, F., Manzano, I., Martín, D., Morín, J., Roquero, E., 2012. Contexto geomorfológico y principales rasgos tecnológicos de nuevos yacimientos del Pleistoceno Medio y Superior en el Valle Inferior del Manzanares (Madrid, España). *Estud. Geol.* 68, 58–89.
- Silva, P.G., Roquero, E., López-Recio, M., Huerta, P., Martínez-Graña, A.M., 2016. Chronology of fluvial terrace sequences for large Atlantic rivers in the Iberian Peninsula (Upper Tagus and Duero drainage basins, Central Spain). *Quat. Sci. Rev.* 166, 188–203.
- Sutton, S.R., Zimmerman, D.W., 1978. Thermoluminescence dating: radioactivity in quartz. *Archaeometry* 20 (1), 67–69.
- Toyoda, S., Falguères, C., 2003. The method to represent the ESR signal intensity of the aluminium hole center in quartz for the purpose of dating. *Adv. ESR Appl.* 20, 7–10.
- Toyoda, S., Voinchet, P., Falguères, C., Dolo, J.M., Laurent, M., 2000. Bleaching of ESR signals by the sunlight: a laboratory experiment for establishing the ESR dating of sediments. *Appl. Radiat. Isotopes* 52 (5), 1357–1362.
- Voinchet, P., Falguères, C., Laurent, M., Toyoda, S., Bahain, J.J., Dolo, J.M., 2003. Artificial optical bleaching of the aluminium center in quartz implications to ESR dating of sediments. *Quat. Sci. Rev.* 22, 1335–1338.
- Voinchet, P., Falguères, C., Tissoux, H., Bahain, J.J., Despriée, J., Pirouelle, F., 2007. ESR dating of fluvial quartz: estimate of the minimal distance transport required for getting a maximum optical bleaching. *Quat. Geochronol.* 2, 363–366.
- Woda, C., Wagner, G.A., 2007. Non-monotonic dose dependence of the Ge- and Ti-Centers in quartz. *Radiat. Meas.* 42 (9), 1441–1452.
- Wolf, D., Seim, A., Díaz del Olmo, F., Faust, D., 2013. Late Quaternary fluvial dynamics of the Jarama river in central Spain. *Quat. Int.* 302, 20–41.
- Yokoyama, Y., Falguères, C., Quaegebeur, J.P., 1985. ESR dating of quartz from quaternary sediments: first attempts. *Nucl. Tracks* 10 (4–6), 921–928.
- Yravedra, J., Domínguez-Rodrigo, M., 2008. The shaft-based methodological approach to the quantification of long limb bones and its relevance to understanding hominid subsistence in the Pleistocene: application to four Palaeolithic sites. *J. Quat. Sci.* 24 (1), 85–96.
- Yravedra, J., Rubio-Jara, S., Panera, J., Uribelarrea, D., Pérez-González, A., 2012. Elephants and subsistence. Evidence of the human exploitation of extremely large mammal bones from the Middle Palaeolithic site of PRERESA (Madrid, Spain). *J. Archaeol. Sci.* 39, 1063–1071.